300mK Strap System

Design Description

Document Ref.: SPIRE-
Cardiff Ref.: HSO-CDF-DD-038
Issue: 2.0

Prepared by: Peter Hargrave
Last Modified on: 12 February 2003
Approved by:

Distribution list

Brian Kiernan	Cardiff	Jamie Bock	JPL
Matt Griffin	Cardiff	Dustin Crumb	JPL
Peter Ade	Cardiff	Hien Nguyen	JPL
Iris Didschuns	Cardiff	Laurent Vigroux	CEA Saclay
Bruce Swinyard	RAL	Lionel Duband	CEA SBT
Eric Sawyer	RAL	Berend Winter	MSSL
John Delderfield	RAL	John Coker	MSSL
Sam Heys	RAL	Chris Brockley-Blatt	MSSL

Update history

Date	Version	Remarks
4th July 2002	1.0	DDR Release
7th February 2003	2.0	Delta-DDR Release. Includes detailed design of bus-bar assembly.

List of Acronyms

Term	Meaning	Term	Meaning
AD	Applicable Document	IR	Infrared
ADC	Analogue to Digital Converter	IRD	Instrument Requirements Document
AIV	Assembly, Integration and Verification	IRTS	Infrared Telescope in Space
AME	Absolute Measurement Error	ISM	Interstellar Medium
AOCS	Attitude and Orbit Control System	JFET	Junction Field Effect Transistor
APART	Arizona's Program for the Analysis of Radiation Transfer	ISO	Infrared Space Observatory
APE	Absolute Pointing Error	LCL	Latching Current Limiter
ASAP	Advanced Systems Analysis Program	LIA	Lock-In Amplifier
ATC	Astronomy Technology Centre, Edinburgh	LVDT	Linear Variable Differential Transformer
AVM	Avionics Model	LWS	Long Wave Spectrometer (an instrument used on ISO)
BDA	Bolometer Detector Array	MAC	Multi Axis Controller
BFL	Back Focal Length	MAIV	Manufacturing, Assembly, Integration and Verification
BRO	Breault Research Organization	MCU	Mechanism Control Unit = HSMCU
BSM	Beam Steering Mirror	MGSE	Mechanical Ground Support Equipment
CBB	Cryogenic Black Body	M-P	Martin-Puplett
CDF	Cardiff, Department of Physics & Astronomy	NEP	Noise Equivalent Power
CDMS	Command and Data Management System	NTD	Neutron Transmutation Doped
CDMU	Command and Data Management Unit	OBS	On-Board Software
CDR	Critical Design Review	OGSE	Optical Ground Support Equipment
CEA	Commissariat a l'Energie Atomique	OMD	Observing Modes Document
CMOS	Complimentary Metal Oxide Silicon	OPD	Optical Path Difference
CoG	Centre of Gravity	PACS	Photodetector Array Camera and Spectrometer
CPU	Central Processing Unit	PCAL	Photometer Calibration source
CQM	Cryogenic Qualification Model	PFM	Proto-Flight Model
CVV	Cryostat Vacuum Vessel	PID	Proportional, Integral and Differential (used in the context of feedback control loop architecture)
DAC	Digital to Analogue Converter	PLW	Photometer, Long Wavelength
DAQ	Data Acquisition	PMW	Photometer, Medium Wavelength
DCU	Detector Control Unit = HSDCU	POF	Photometer Observatory Function
DDR	Detailed Design Review	PROM	Programmable Read Only Memory
DM	Development Model	PSW	Photometer, Short Wavelength
DPU	Digital Processing Unit = HSDPU	PUS	Packet Utilisation Standard
DSP	Digital Signal Processor	RAL	Rutherford Appleton Laboratory,
DQE	Detective Quantum Efficiency	RD	Reference Document
EDAC	Error Detection and Correction	RMS	Root Mean Squared
EGSE	Electrical Ground Support Equipment	SCAL	Spectrometer Calibration Source
EM	Engineering Model	SCUBA	Submillimetre Common User Bolometer Array
EMC	Electro-magnetic Compatibility	SED	Spectral Energy Distribution
EMI	Electro-magnetic Interference	SMEC	Spectrometer Mechanics
ESA	European Space Agency	SMPS	Switch Mode Power Supply
FCU	FCU Control Unit = HSFCU	SOB	SPIRE Optical Bench
FIR	Far Infrared	SOF	Spectrometer Observatory Function
FIRST	Far Infra-Red and Submillimetre Telescope	SPIRE	Spectral and Photometric Imaging Receiver
FOV	Field of View	SRAM	Static Random Access Memory
F-P	Fabry-Perot	SSSD	SubSystem Specification Document
FPGA	Field Programmable Gate Array	STP	Standard Temperature and Pressure
FPU	Focal Plane Unit	SVM	Service Module
FS	Flight Spare	TBC	To Be Confirmed
FTS	Fourier Transform Spectrometer	TBD	To Be Determined
FWHM	Full Width Half maximum	TC	Telecommand
GSFC	Goddard Space Flight Center	URD	User Requirements Document
HK	House Keeping	UV	Ultra Violet
HOB	Herschel Optical Bench	WE	Warm Electronics
HPDU	Herschel Power Distribution Unit	ZPD	Zero Path Difference
HSDCU	Herschel-SPIRE Detector Control Unit		
HSDPU	Herschel-SPIRE Digital Processing Unit		
HSFCU	Herschel-SPIRE FPU Control Unit		
HSO	Herschel Space Observatory		
IF	Interface		
IID-A	Instrument Interface Document - Part A		
IID-B	Instrument Interface Document - Part B		
IMF	Initial Mass Function		

Table of Contents

List of Figures

1. Scope

This document describes the design of the Herschel-SPIRE 300mK strap subsystem. The intention of this document is to present all design information available at a given release date and will be updated as and when changes to the design are made under configuration control.

2. Documents

2.1. Applicable documents

	Title	Author	Reference
AD1	Instrument Requirements Document	B.M. Swinyard	SPIRE-RAL-PRJ-000034 Issue 0.30
AD2	SPIRE Thermal Configuration Control Document	S. Heys	SPIRE-RAL-PRJ-000560, Issue D9
AD3	SPIRE Structural Mechanical I/F	B. Winter	MSSL/SPIRE/SP004.12

2.2. Reference documents

	Title	Author	Reference
RD1	SPIRE 300-mK Strap System Development Plan	D. Griffin	SPIRE-RAL-PRJ-001317
RD2	A stray-light baffle design for thermal strap entry ports	A G Richards	SPIRE-RAL-NOT-000344
RD3	Herschel/SPIRE 300mK strap system requirements	D. Griffin	SPIRE-RAL-PRJ-001323
RD4	Herschel-SPIRE Interface Control Document (BDA ICD)		JPL Document D-21995
RD5	FEA of 300mK Thermal Strap System	B.Winter	MSSL-technote-SPIRE-18
RD6	300mK thermal interface test summary	I.Didschuns	Cardiff tech. note. HSO-CDF-RP-xxx

3. Overview of 300mK strap system

The 300mK strap system links the ^{3}He cooler tip with all five detector arrays in the SPIRE instrument. The straps must have a high degree of thermal isolation from warmer structure while at the same time be able to withstand high levels of launch vibration with very high reliability. In order to fulfill these somewhat conflicting requirements, a Kevlar suspension system has been developed to support the 300mK straps. An additional complication is the fact that the thermal interfaces for the 300mK straps to the detectors are inside the Level-0 detector boxes at approximately 2K. The 300mK straps pass from the Level-1 (~4K) environment of the cooler tip, through the Level-0 detector box walls, into the ~2K environments of the photometer and spectrometer detector boxes. Therefore a light baffle has been developed, based on the Kevlar support idea, which supports the straps as they pass through the detector box walls, while at the same time providing a high degree of stray light attenuation.

Error! Objects cannot be created from editing field codes.

Figure 1 Block diagram of 300mK strap system. The straps are shown in dark blue, and thermal interfaces to other subsystems are shown as blue circles. PSUP1 and PSUP2 are the photometer strap supports, and PBAF & SBAF are the photometer & spectrometer supports/light baffles.

4. Detailed Design Description

4.1. Design Drivers

4.1.1. Reliability

The 300mK strap system has the potential to provide a single point failure for the whole of the SPIRE instrument. All five detector arrays are linked via the 300mK straps to the single cooler tip. If any part of the strap system fails and produces a thermal short to the warmer structure, depending upon the severity of the short, all detectors may rise beyond any useful operating temperature. Therefore reliability has the utmost importance in the sub-system design, at the expense of any other design driver.

4.1.2. Thermal Isolation

The total budget allocated for parasitic heat load to the cooler from the 300mK strap system is 2.0μW. Analysis and preliminary thermal tests show that the design presented in this document for the suspension of the straps meets this requirement with reasonable margin.

4.1.3. Light Tightness

The detector arrays are mounted to the Level-0 detector boxes on the photometer and spectrometer. The 300mK strap/detector interface is on the front face of each BDA, i.e. on the inside of each Level-0 box. Therefore the 300mK straps must be brought from a Level-1 environment at approximately 4K, through the photometer and spectrometer box walls, into the ~2K environment. The feedthroughs must serve the

dual purpose of providing thermally isolating support and a high level of stray light attenuation.
This design driver has lower priority than 4.1.1 (reliability) - mechanical integrity will not be compromised for the benefit of improved light-tightness (see RD2)

4.1.4. Stiffness

The first mode of the 300mK system should be as high as possible (RD1) in order to avoid transmitting additional mechanical loads to the BDAs or cooler tip.

4.2. Photometer Strap Suspension

There are two identical bus-bar supports within the photometer box. These supports provide a high degree of thermal isolation and mechanical strength by the use of Kevlar under tension, as shown in Figure 2. The main body of each support is bolted to the photometer box lid at 2K, and there is a central hub, which carries the 300mK bus-bar axially. This central hub is made in two sections; part of one section fits concentrically inside the other so that the whole hub can expand telescopically. A stack of Belleville spring washers between the hub sections is used to provide resistance to compression. The central hub assembly is compressed before the whole assembly is “laced” with the Kevlar. The Kevlar is pre-tensioned and terminated at two sets of capstans. Throughout this process, jigs are in place to ensure correct alignment of the central hub with respect to the support body. The compression of the central hub is then released and the alignment jigs are removed. The result is a well-aligned, modular, stiff thermal isolation unit, ready for integration with the rest of the 300mK strap system.

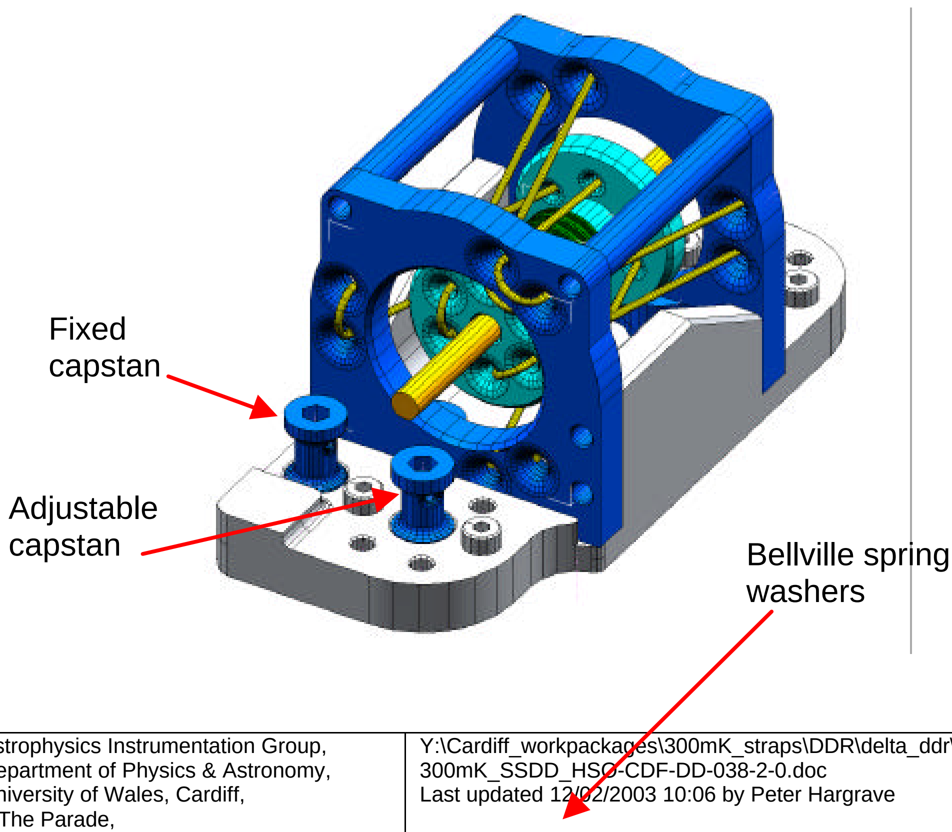

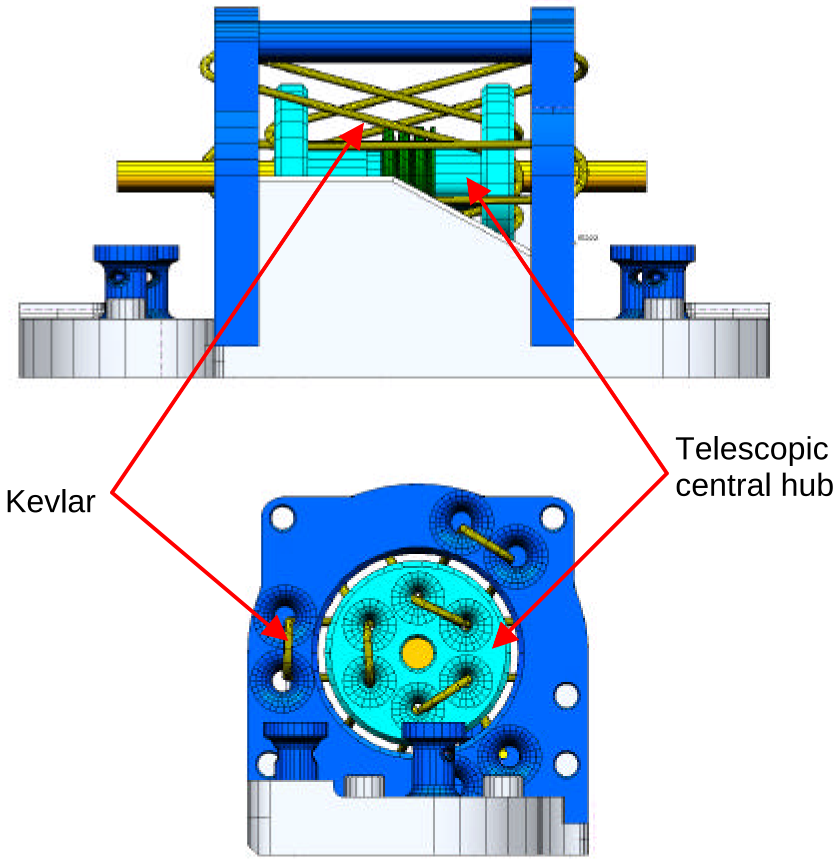

Figure 2 Views of a photometer 300mK strap support module

4.2.1. Kevlar type

Prototype devices used 167 Tex Kevlar fibre bundles from Goodfellow PLC (1 Tex = 1 gram/km). Although very strong, there is no real "containment" of the individual fibres as they all run parallel to each other. The flight devices will use Kevlar "ropes" of the type currently being qualified for the SPIRE ^{3}He cooler. The bulk material comes from Dupont de Nemours, and is formed into "ropes" by Cousin-Filterie, a company located in the north of France (Cousin filterie, 8 rue Abbé Bonpain, BP 6 Wervicq Sud, 59558 Comines Cedex). An example of this "rope" is shown in Figure 3.

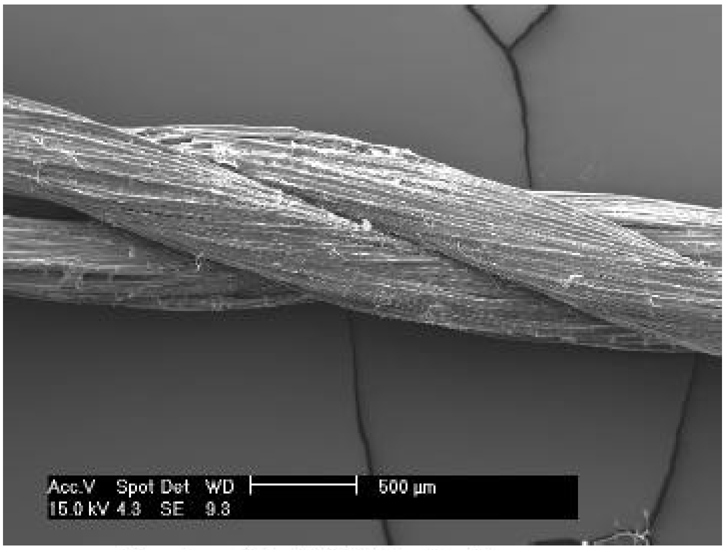

Kevlar 11 (80°C baked)

Figure 3 Kevlar "rope" for 300mK strap suspension

For this application, we take advantage of the following properties of Kevlar:-

- High tensile strength
- High Young's modulus
- Low thermal conductivity at low temperature

A comparison between Nylon, stainless steel, Titanium Ta6V and Kevlar is shown in Table 1. As a first approximation the goal is to maximise the resonant frequencies (proportional to the square root of the Young's modulus "Y ")and the strength "σ ", and to minimise the thermal load (proportional to the integrated thermal conductivity "I " between say 0.3 and 2 K).

Table 1 Comparison of thermal isolation materials – extracted from Ref [1].

	Nylon	Stainless	Titanium Ta6V	Kevlar 29
σ (MPa)*	100	550	875	1600
Y (MPa)*	3 000	200 000	110 000	65 000
I (W/cm)	$5.9\ 10^{-5}$	$2\ 10^{-3}$	10^{-3}	$7\ 10^{-5}$
$\sigma.Y^{0.5}/I$	$0.9\ 10^{8}$	$1.2\ 10^{8}$	$2.9\ 10^{8}$	$58\ 10^{8}$

(*: mechanical properties at ambiant temperature)

Kevlar also has a few disadvantages which are accounted for in the design:-

- The fibres absorb moisture. All support and light baffle assemblies will be vacuum baked and stored in a dessicator when not in use, prior to integration with SPIRE.
- Although the tensile strength and modulus is high, compressive properties are relatively poor. This has been taken into account in the design of the capstans and the Kevlar routing.
- Kevlar is susceptible to "creep" which manifests itself to a small increase in length over a long time period.
- Kevlar has a small negative longitudinal thermal expansion coefficient – it gets longer as it cools down. This point, and the previous one, is addressed by the design of the telescopic central hub. A stack of Belleville spring washers

maintains tension by causing a slight increase in the length of the hub, which will compensate for any cord expansion,

4.2.2. Kevlar routing

The routing of the Kevlar is shown in Figure 4. Two independent cords are used, although this does not add redundancy. Both cords are needed to maintain tension. An important design feature of the support module is that the Kevlar cord is never threaded around a bend diameter less than 4mm. Duband [1] has shown that a bend diameter greater than 3mm is required for Kevlar passing around a pulley or capstan under tension if the full rated strength of the cords is to be achieved. In other words, below a diameter of 3mm, stress concentrations build up and weaken the Kevlar at these points, as shown in Figure 5.

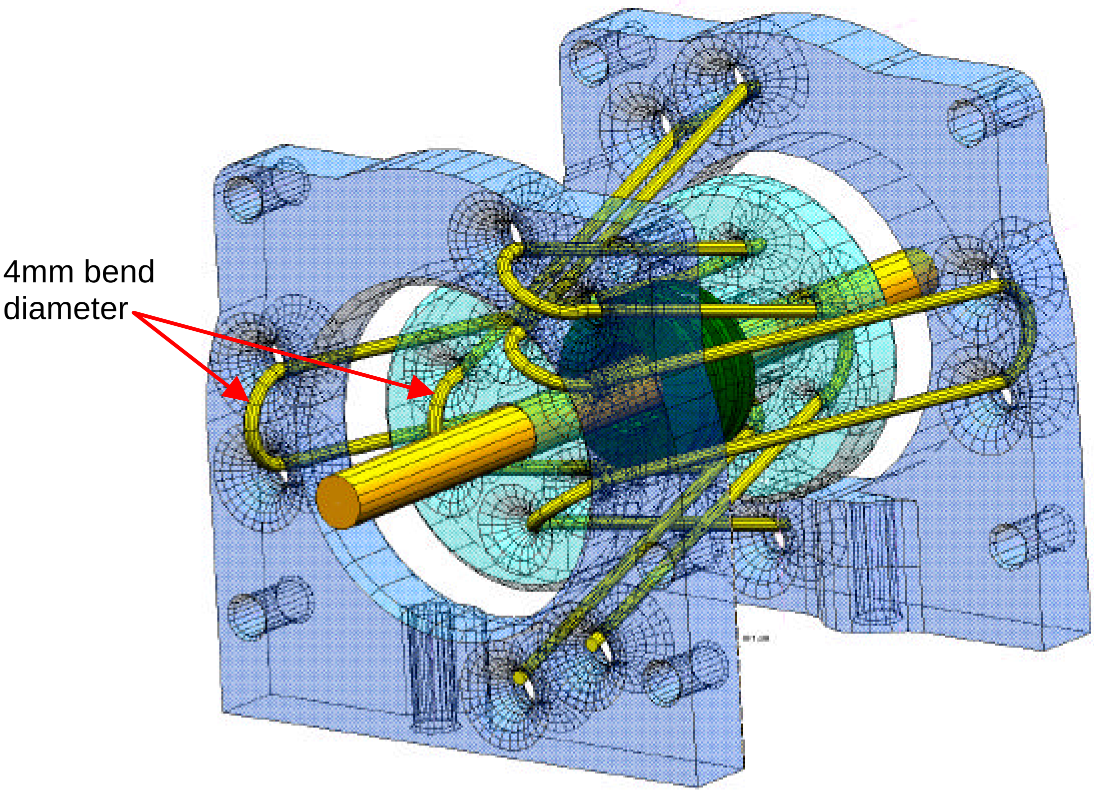

Figure 4 Kevlar routing for photometer bus-bar support

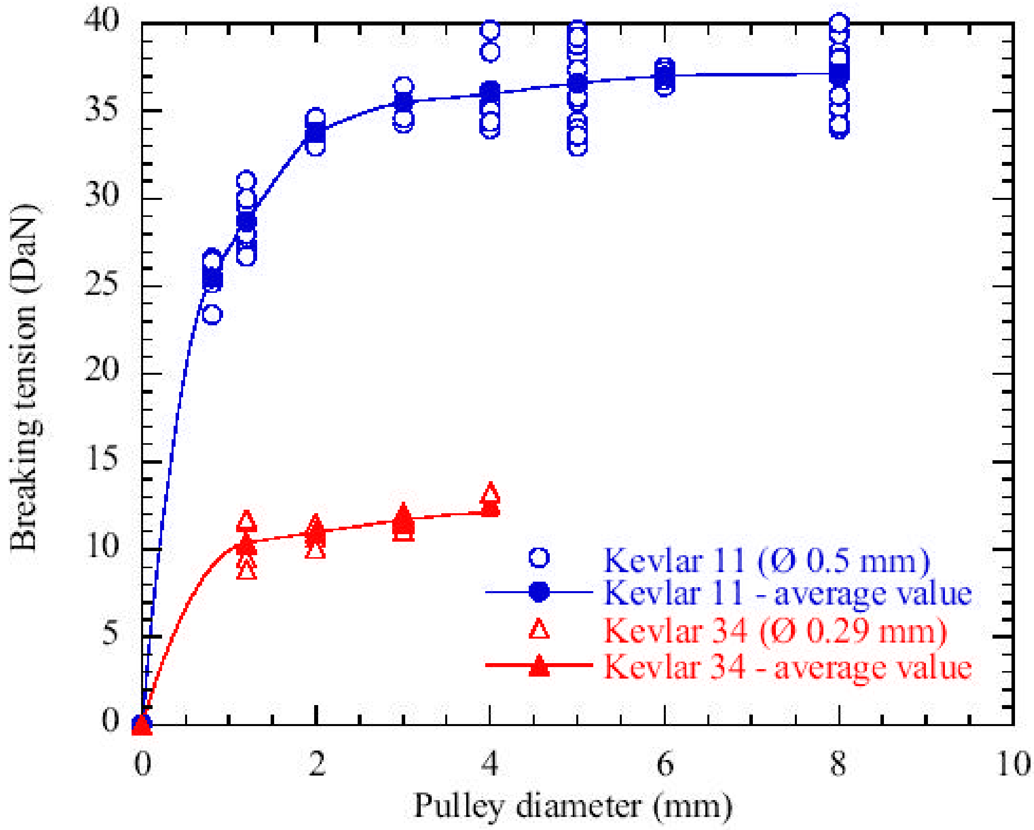

Figure 5 Kevlar breaking strength as a function of pulley diameter (from Ref. [1])

4.2.3. Capstans

Termination of the Kevlar was a potential problem. Any direct knot in the Kevlar must be avoided, as the fibres would tend to cut into each other and producing a weak spot at the knot. Duband [1] showed that the presence of a knot weakens the Kevlar by approximately 50%. Therefore this design employs capstans, again following the recommendations in Ref. [1]. The idea behind the capstan is that the "residual tension", proportional to the number of turns around the capstan, can be lowered to a level where a knot can be used without weakening the termination. This is shown by a simple experiment carried out by Duband. The Kevlar cord is permanently loaded on one side, then goes around a capstan by "n" turns, and is attached to a force transducer on the other side (Figure 6). Figure 7 shows how the remaining tension is affected by the number of turns around the capstan.
A second experiment used a capstan with a hole in which one end of the Kevlar cord is inserted and locked with a knot, and the cord then wound around the capstan by "n" turns. Figure 8 shows the breaking strength of this arrangement as a function of the number of turns around the capstan. These results show that a cord arrangement featuring at least 3 turns around the capstan allows the remaining tension at the end of the cord to be lowered to such a level where a knot may be safely employed. A concern is slippage of the cord around the capstan, effectively increasing the tension in the region of the knot. Duband has tested for this effect and found no increase in the "residual tension" after 4 days (using 3 capstan turns). A long term fatigue

behaviour experiment has been started at SBT to test thoroughly for this, and other, effects.

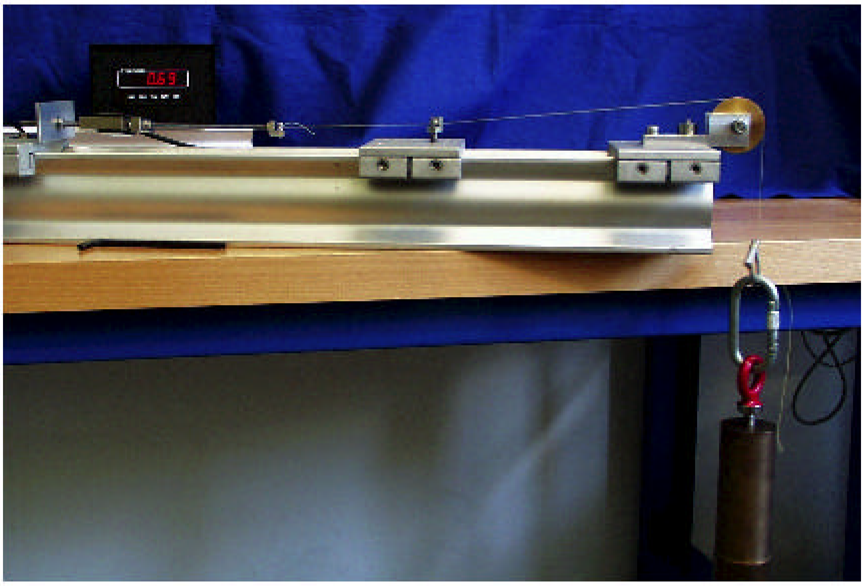

Figure 6 Experimental arrangement for capstan tests.

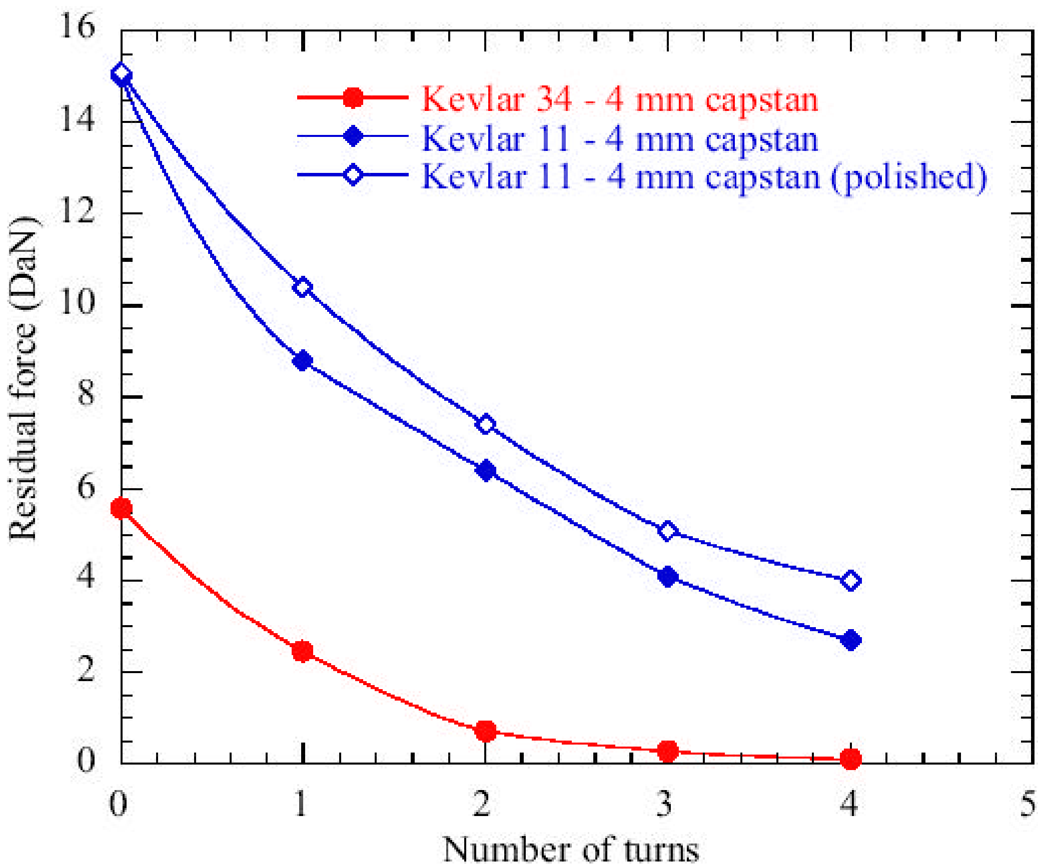

Figure 7 Residual force as a function of number of capstan turns

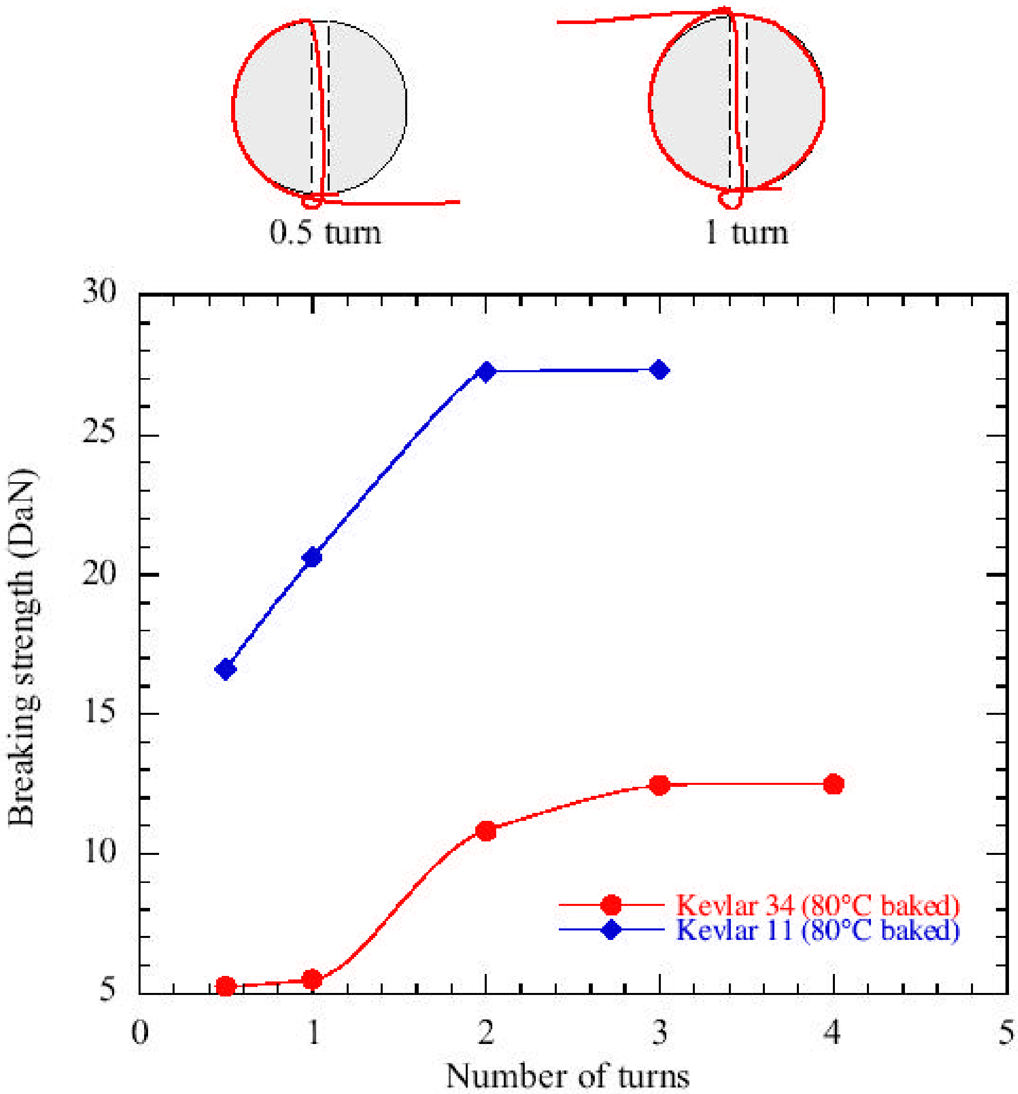

Figure 8 Breaking strength as a function of number of turns around capstan.

The knots used at the capstans are adjustable jam hitches, illustrated in Figure 9. This type of knot is used, as it tends to tighten under tension without imparting undue compressive stress on the Kevlar cord.

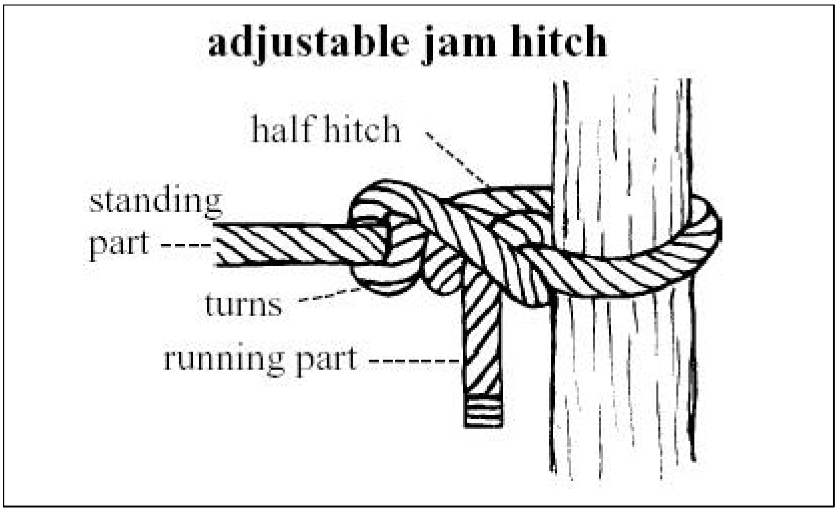

Figure 9 Details of knot used for terminating the Kevlar at capstans.

4.2.3.1. Capstan details

For each support assembly, there are two Kevlar cords. Each cord employs two capstans. The cord run starts on a fixed capstan and ends on an adjustable capstan, details of which are shown in Figure 10.

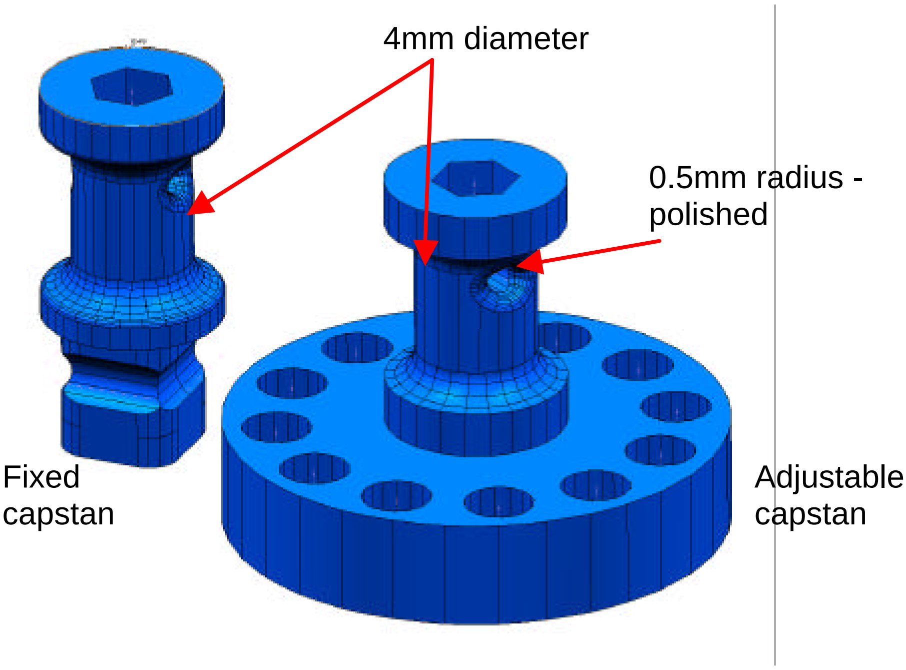

Figure 10 Details of capstans for photometer 300mK bus-bar supports.

The adjustable capstan has twelve threaded holes with locking inserts, and in combination with the six holes on the baseplate (two of which are used at any one time) provides adjustment steps of 7.5°. A minimum of four turns around each capstan is used for the Kevlar rope.

4.2.4. Hub assembly

The hub assembly consists of the two stainless steel parts of the hub itself, together with a stack of Belleville spring washers and the optional use of a spacer ring to replace some of the washers, as shown in Figure 11 and Figure 12. The two hub parts interlock and one is able to slide over the other to form a telescopic hub. The Belleville washers can be stacked in a variety of ways (series, parallel, series/parallel combination) to provide the desired compressibility range and restoring force.

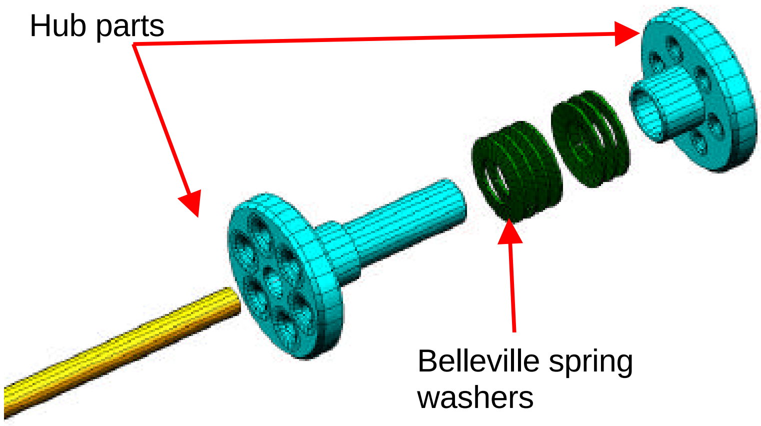

Figure 11 Exploded view of hub assembly

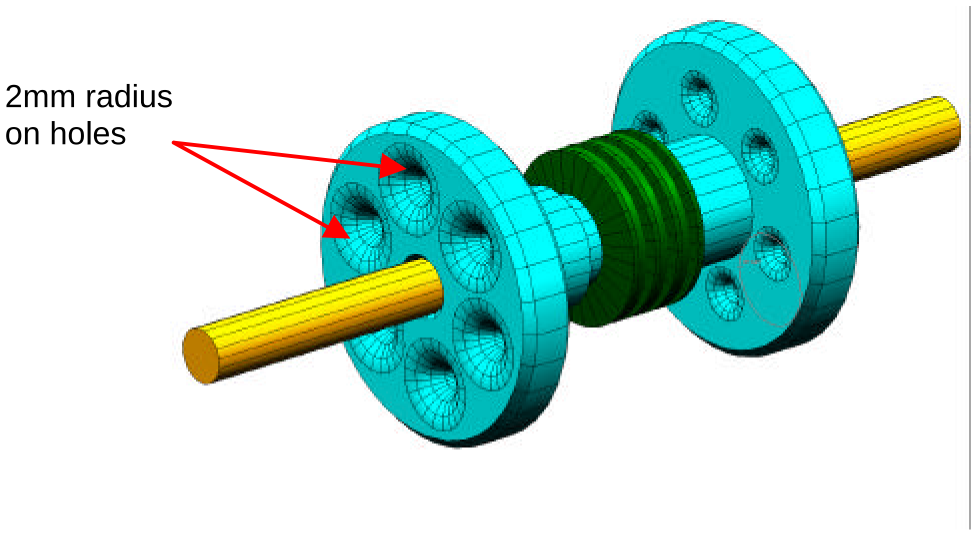

Figure 12 Hub assembly with bus-bar

4.2.4.1. Belleville spring washers

Stainless steel disc spring washers (Belleville springs LTD, Worcestershire) are employed to tension the Kevlar by forcing the central hub to expand. The spring washers can be stacked in various ways to obtain the desired range of deflection and restoring force, as shown in Figure 13. The central hub has been designed to accommodate up to eight series-stacked washers, more if series-parallel stacked. If less than eight are used, or some are stacked in parallel, the excess length is taken up with a pair of spacer rings.

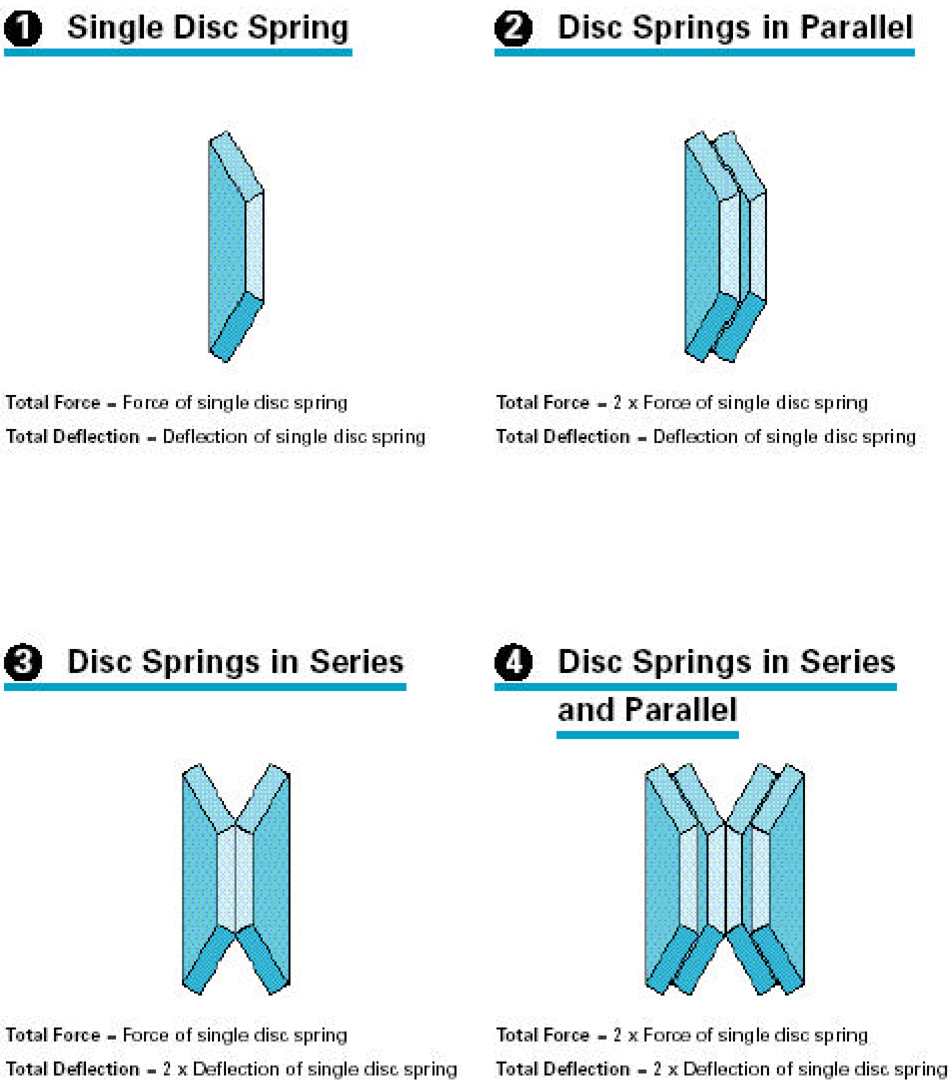

Figure 13 Options for stacking disc spring washers.

The disc spring type selected for the telescopic hub is part number S105204, data for which is shown in Table 2. The hub is compressed such that the disc spring compression is ~90%, prior to suspending the hub on the Kevlar. This is achieved by using an M3 bolt and nut through the central axis, with the nut turned to a torque specified in the assembly procedure (depends on Bellville stacking pattern). The Kevlar is then pulled taut to a fixed pre-load and terminated at the capstans. Then the external compression of the hub is released, and the restoring force of the Belleville stack will fully tension the Kevlar. This tension is determined by the Belleville stacking arrangement, and the pre-compression applied. Tests have been carried out on an STM prototype device which employed twelve series-parallel stacked washers (stacking pattern = <<<>>><<<>>>) with 90% initial compression, and an initial Kevlar tension (prior to hub release) set by winding the Kevlar cords onto the adjustable capstans to a torque of 60±5 Ncm.

Table 2 Data for stainless steel disc springs for use in telescopic hub.

Stainless Disc Springs

Material: X12CrNi 17 7 (DIN 1.4310)

Code No.	Outer Dia. (De) mm	Inner Dia. (Di) mm	Thick. (t) mm	Cone Ht. (ho) mm	Overall Ht. (lo) mm	Cone Ht. / Thick. Ratio	Weight per 1000 pcs.
S63203	6.0	3.2	.30	.15	.45	.50	.05
S63205	8.0	3.2	.51	.20	.70	.40	.17
S84202	8.0	4.2	.20	.25	.45	1.25	.06
S84203	8.0	4.2	.30	.25	.55	.83	.09
S84204	8.0	4.2	.41	.20	.60	.50	.11
S1062025	10.0	5.2	.25	.30	.55	1.20	.11
S106204	10.0	5.2	.40	.30	.70	.75	.18
S106205	10.0	5.2	.50	.25	.75	.50	.22

Code No.	15% Defl. Defl. mm / Stress σ_{II} N/mm²	15% Defl. Force N / Stress σ_{III} N/mm²	30% Defl. Defl. mm / Stress σ_{II} N/mm²	30% Defl. Force N / Stress σ_{III} N/mm²	45% Defl. Defl. mm / Stress σ_{II} N/mm²	45% Defl. Force N / Stress σ_{III} N/mm²
S63203	.02	25	.05	49	.07	70
	183	252	387	490	612	714
S63205	.03	72	.06	141	.09	206
	276	229	572	448	889	655
S84202	.04	13	.08	22	.11	29
	-6	233	20	445	79	636
S84203	.04	30	.08	55	.11	76
	91	384	215	548	371	789
S84204	.03	45	.06	85	.09	124
	183	247	387	481	612	702
S1062025	.05	18	.09	32	.14	42
	2	217	34	414	96	592
S106204	.05	51	.09	95	.14	132
	114	275	258	531	432	767
S106205	.04	69	.08	133	.11	192
	183	345	387	477	612	695

Code No.	60% Defl. Defl. mm / Stress σ_{II} N/mm²	60% Defl. Force N / Stress σ_{III} N/mm²	75% Defl. Defl. mm / Stress σ_{II} N/mm²	75% Defl. Force N / Stress σ_{III} N/mm²	90% Defl. Defl. mm / Stress σ_{II} N/mm²	90% Defl. Force N / Stress σ_{III} N/mm²
S63203	.09	91	.11	110	.14	129
	958	924	1,125	1,121	1,413	1,304
S63205	.12	269	.15	330	.18	389
	1,226	851	1,584	1,036	1,962	1,210
S84202	.15	33	.19	36	.23	38
	170	806	294	954	461	1,081
S84203	.15	94	.19	109	.23	122
	560	1,010	782	1,210	1,036	1,388
S84204	.12	159	.15	193	.18	226
	857	908	1,124	1,102	1,411	1,281
S1062025	.18	49	.23	53	.27	56
	188	751	309	890	461	1,010
S106204	.18	164	.23	193	.27	220
	636	984	870	1,181	1,134	1,359
S106205	.15	247	.19	300	23	351
	857	899	1,123	1,090	1,411	1,268

4.2.4.2. Kevlar pre-tension and spring stacking options

There are many options for pre-tensioning the Kevlar by using different arrangements of spring washers, as shown in Table 3. In this table, D_T is the total stack deflection for an individual washer deflection of 75% or 90%, F is the restoring force from the stack, and T_K is the resulting tension in each Kevlar cable (twelve per support assembly). The predicted breaking stress for each Kevlar cable is around 500 N.

Table 3 Options for adjusting the Kevlar pre-load using different Bellville spring washer configurations

Belleville spring configuration	Belleville deflection					
	75%			90%		
	D_T(mm)	F (N)	T_K(N)	D_T(mm)	F (N)	T_K(N)
8 series	*1.84*	*193*	*16.3*	*2.16*	*220*	*18.5*
8 series/parallel (4 pairs)	*0.92*	*386*	*32.5*	*1.08*	*440*	*37.1*
8 series/parallel (2 nests of 4)	*0.46*	*772*	*65.1*	*0.54*	*880*	*74.2*
12 series/parallel (4 nests of 3)	*0.92*	*579*	*48.8*	*1.08*	*660*	*55.6*

The Belleville configuration to be used for the STM/CQM photometer supports and light baffles is as indicated in the last row of Table 3. This should give a final tension in each Kevlar cable length of around 56 N (initial compression of 90%).

4.3. Light Baffles

All five detector array modules are mounted on the 2K photometer and spectrometer detector boxes. The feedhorn apertures look into the low-background 2K environments of these light-tight boxes. A low-pass edge filter covers the entrance apertures of these boxes. The detector interface for the 300mK strap is on the front face of each BDA, which means that the 300mK bus-bar must be brought into each 2K box while retaining a high level of light-tightness. Of course, there cannot be any direct contact between the 300mK components and the 2K boxes. Therefore a light-trap has been designed which provides a rigid support, a high degree of thermal isolation, and a reasonable level of stray light attenuation. General views of the assembled baffle are shown in Figure 14, and an illustration of one of the baffles in place on the photometer 2K box is shown in Figure 15.

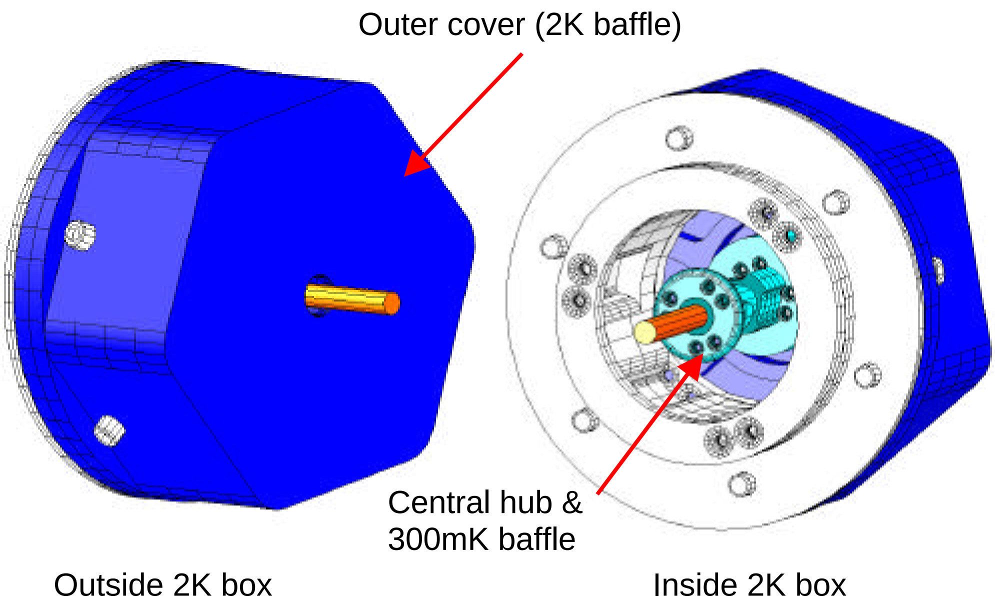

Figure 14 General views of the light baffle assembly

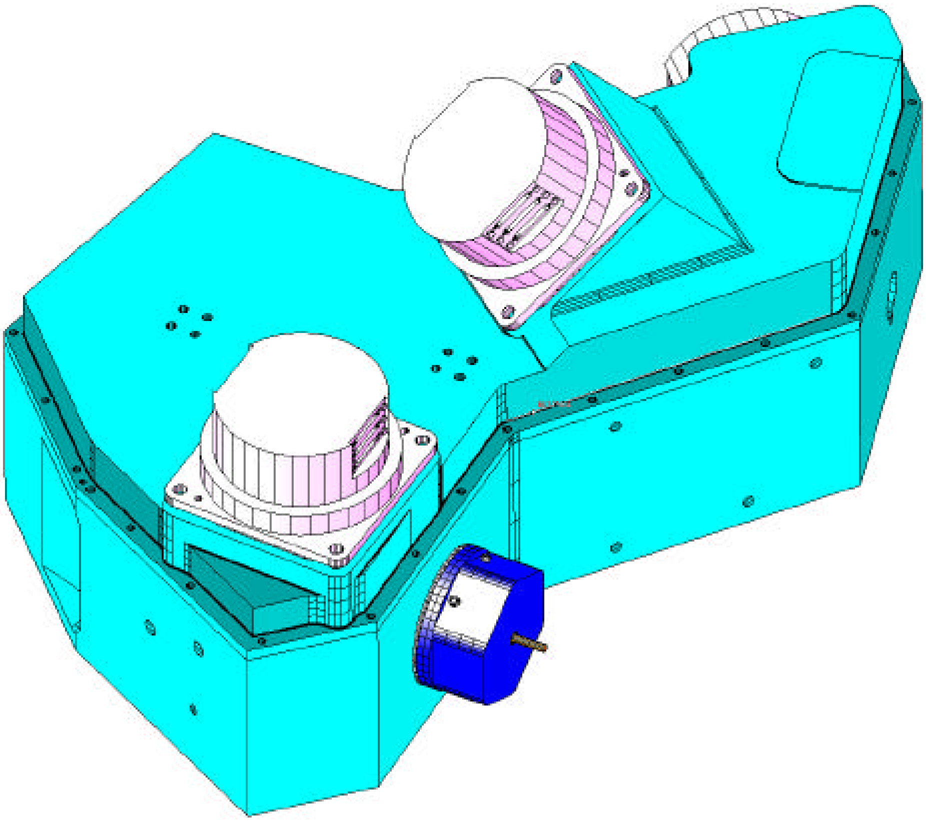

Figure 15 Light baffle in position on the photometer box spine. An identical baffle is employed on the spectrometer 2K box.

4.3.1. General assembly

The core of the light baffle assembly is essentially the same as the photometer bus-bar support. It employs a Kevlar suspension system with a Belleville-tensioned telescopic central hub. Concentric, overlapping tubular baffles form a light trap – one on the central hub (300mK section) and two on the light baffle cover at ~2K.

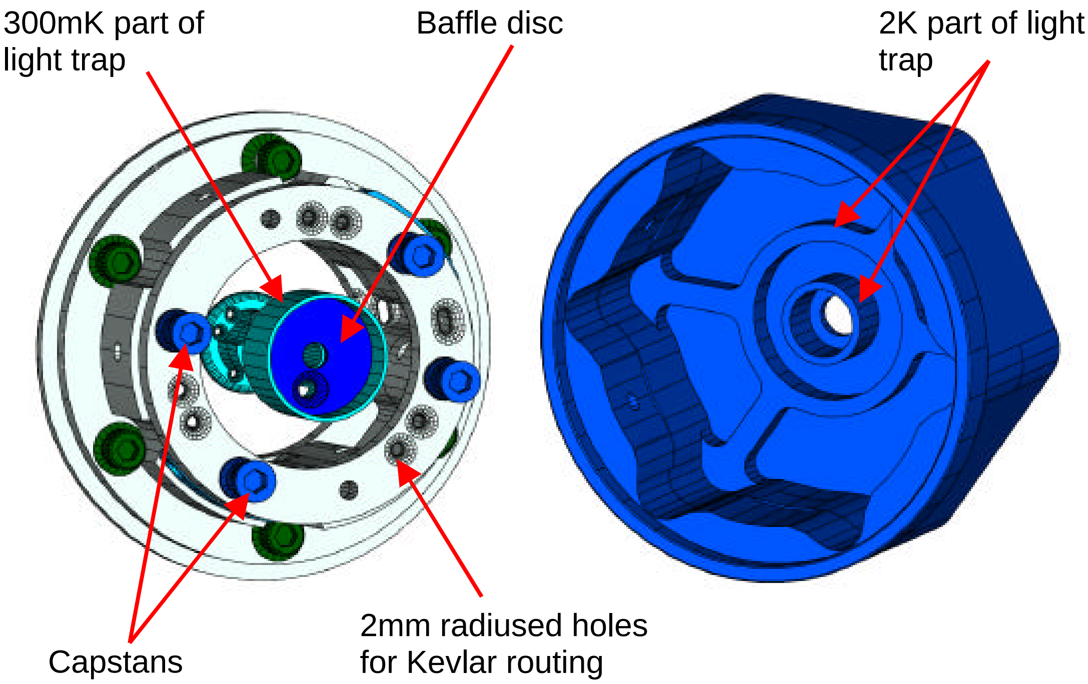

Figure 16 Light baffle assembly – outer cover removed. Baffle disc is used to cover Kevlar routing holes on central hub.

4.3.2. Light baffle design

In designing the light trap, efficacy of light attenuation was considered a less important design driver than avoidance of thermal shorts. Making the individual tube baffle sections tall, with small clearances between baffles (the way to optimize light attenuation – maximize number of photon "bounces") greatly increases the risk of a thermal short from 300mK to Level-0 by misalignment of the hub. Therefore, relatively short tube baffle sections with generous clearances between sections have been employed. Sectional views are shown in Figure 17 and Figure 18. The surfaces of the light trap, and the inside of the light baffle cover, will be coated with a highly absorbent black coating which is currently being qualified at Cardiff for use on SPIRE. A stray light analysis of this arrangement will be carried out, and the level of light leakage will be tested experimentally on the DM devices (built at the same time as the STM/CQM devices).

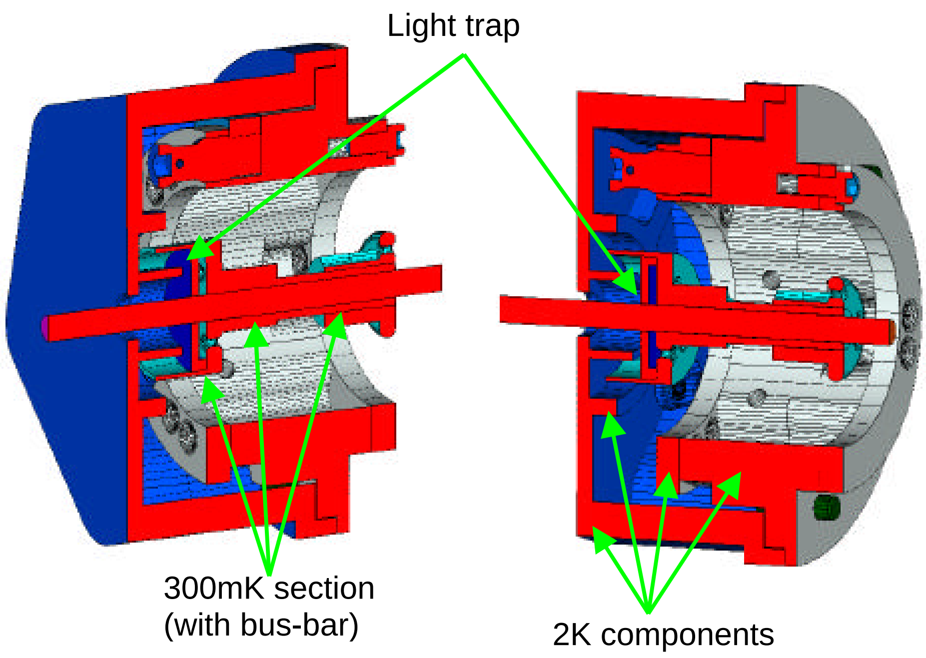

Figure 17 Sectional view of light baffle with bus-bar.

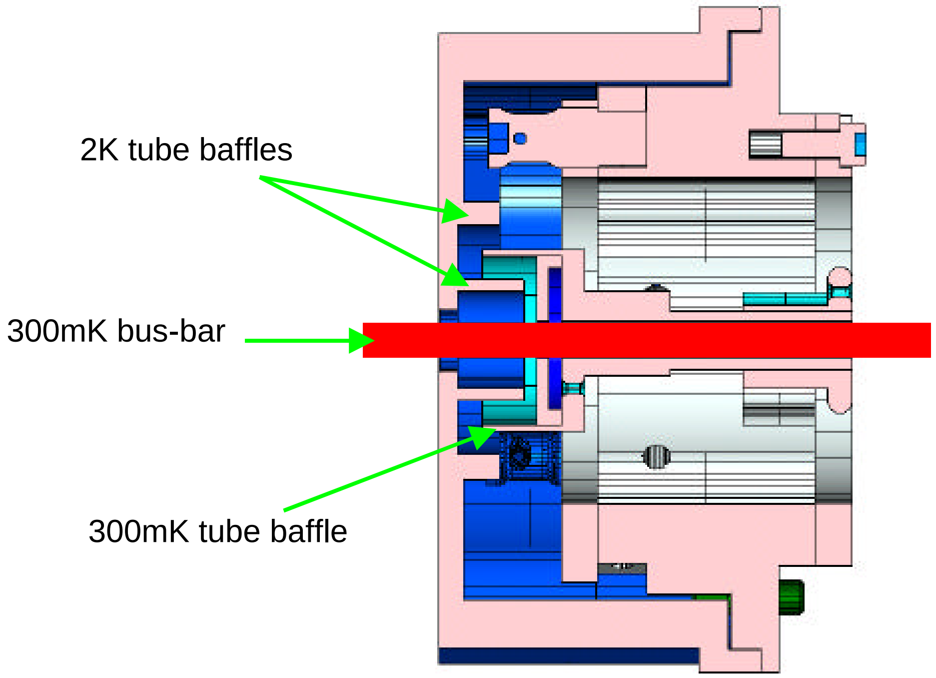

Figure 18 Sectional view showing details of light trap. Minimum clearance between 2K and 300mK structure is 2mm. Blue areas indicate where the black coating will be applied.

4.3.3. Light attenuation requirements

The optical requirements on the stray light baffles are shown in Table 4.

Table 4 Optical requirements on stray light baffles – extracted from RD3

Requirement ID	Description	Value	Reference	Notes
STRAP-Req-18	Stray-light baffling effectiveness	The Photometer and Spectrometer Stray-Light Baffles are to provide at least four reflections for the shortest optical path between the Level-1 environment outside the detector box and the Level-0 environment inside the detector boxes.	IRD-STRP-R06 IRD-STRS-R06. [AD1]	These requirements on the stray-light shielding in terms of attenuation have in terms of been changed into geometric requirements. See RD02
STRAP-Req-19	Stray-Light Baffle Opacity	The Photometer and Spectrometer Stray-Light Baffles are to be opaque (>99.9%) in the wavelengths 0.5µm to 670µm	IRD-STRP-R06 IRD-STRS-R06. [AD1]	Since the attenuation requirement in the IRD has been translated into a geometric requirement, the opacity of the stray light baffle needs to be specified as well.

4.3.3.1. STRAP-Req-18

Because of the greater emphasis put on ensuring adequate clearance between 300mK and Level-0 structure within the light trap, it may prove difficult to fulfill this requirement. A full stray light analysis of the baffles has yet to be carried out at the time of writing, but a naïve analysis shows the potential for a stray light path for which a photon would undergo only three bounces, as shown in Figure 19.

4.3.3.2. STRAP-Rep-19

This requirement for opacity of the light baffles in the wavelength range 0.5µm to 670µm will be easily met, as the baffle is manufactured from aluminium with a minimum thickness of 1mm. The reason for the 0.5µm lower limit is due to the emission of the LED used on the SMEC position sensor (peak at ~1µm).

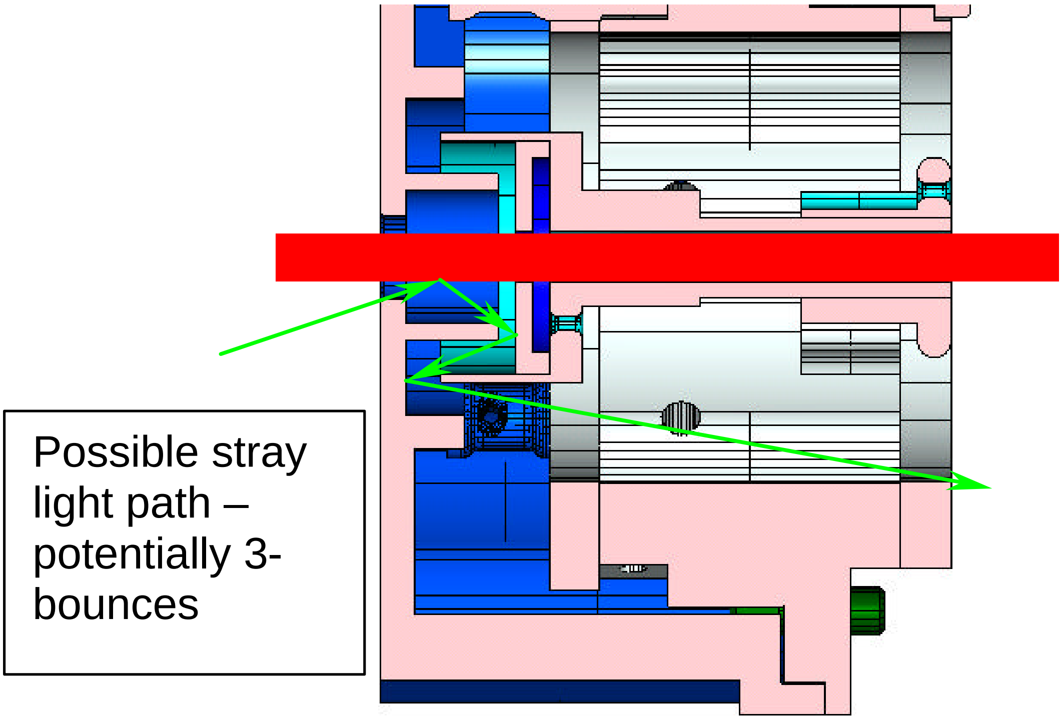

Figure 19 Potential for a "3-bounce" stray light path – unconfirmed.

4.3.4. Light baffle capstans

The Kevlar is terminated on capstans of a similar design to those used for the photometer bus-bar supports. There is a lower range of angular adjustment on the adjustable capstan, due to severe space constraints.

4.4. Mechanical analysis

A full FEA analysis of the 300mK strap system has been carried out, and may be found in RD5.

4.5. Thermal analysis

A thermal model of the Kevlar suspension systems has been produced as a design tool in order to ascertain the level of parasitic heat load to the cooler as a function of Kevlar geometry. A summary of the results for the design presented in this document follows.

4.5.1. Assumptions

- Kevlar type
    - 291 Tex – effective cross-sectional area of $1.97\times10^{-7}m^2$
- Kevlar Conductivity
    - Model run for two conductivity estimates
        - Duband [2]
        - Ventura [3]

- o Venturas data gives the more pessimistic result, and Dubands 300mK conductivity estimate was extrapolated from 2K data. Therefore Venturas data is used for estimation of parasitics.
- Kevlar geometry
  - o Individual cable length (between Level-0 and 300mK) – 25mm
  - o 48 cables from Level-0 to 300mK – twelve per support/light baffle – two photometer strap supports and two light baffles (one each for photometer and spectrometer boxes)
- Level-0 temperature – For estimation of parasitics, a Level-0 temeperature of 2K has been assumed, although in flight, it could be as low as 1.8K [AD2].

4.5.2. Results

The results from this model are shown in Table 5 and Figure 20. The graph plotted in Figure 20 is derived using the Ventura model, which gives the more pessimistic result.

Table 5 Parasitic heat load estimates as a function of Level-0 temperature.

Level-0 temperature	Parasitic load to cooler tip from 300mK strap suspension (μW)	
	Duband model	Ventura model
1.8K	1.42	2.65
2.0K	1.87	3.54

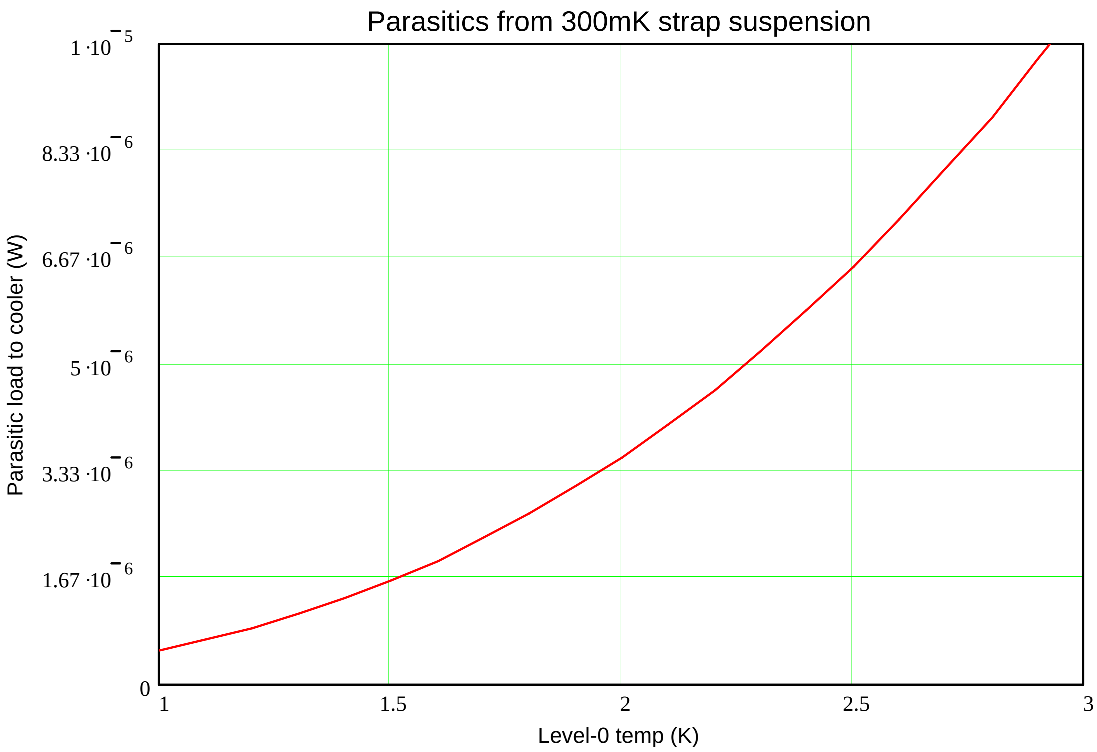

Figure 20 Total parasitics to cooler tip from strap suspension, as a function of Level-0 temperature (from Ventura model).

4.6. *Photometer strap assembly*

4.6.1. System overview

The photometer strap assembly consists of several components. The best situation from a thermal perspective would be have the entire strap assembly formed out of one piece of copper, to minimize the number of thermal interfaces. However, this is obviously impractical due to cost and integration limitations. Therefore the strap system has been designed to allow reasonable integration and ease of manufacture, while keeping the number of thermal interfaces to a minimum.

This means that the photometer strap assembly is split into six components, as illustrated in Figure 21. All components of the strap assembly are manufactured from 99.999% copper (gold-plated), and are identified as follows:-

1) Feed from cooler tip to outside of light baffle.
2) Light baffle feed-through and section 1 of bus-bar – 3mm diameter copper rod.
3) Compliant link to PSW BDA – 1mm dia. copper.
4) Compliant link to PMW BDA – also serves as clamp to section 2 of bus-bar.
5) Section 2 of bus-bar – fed through both photometer strap supports – 3mm dia. copper rod.
6) Compliant link to PLW BDA.

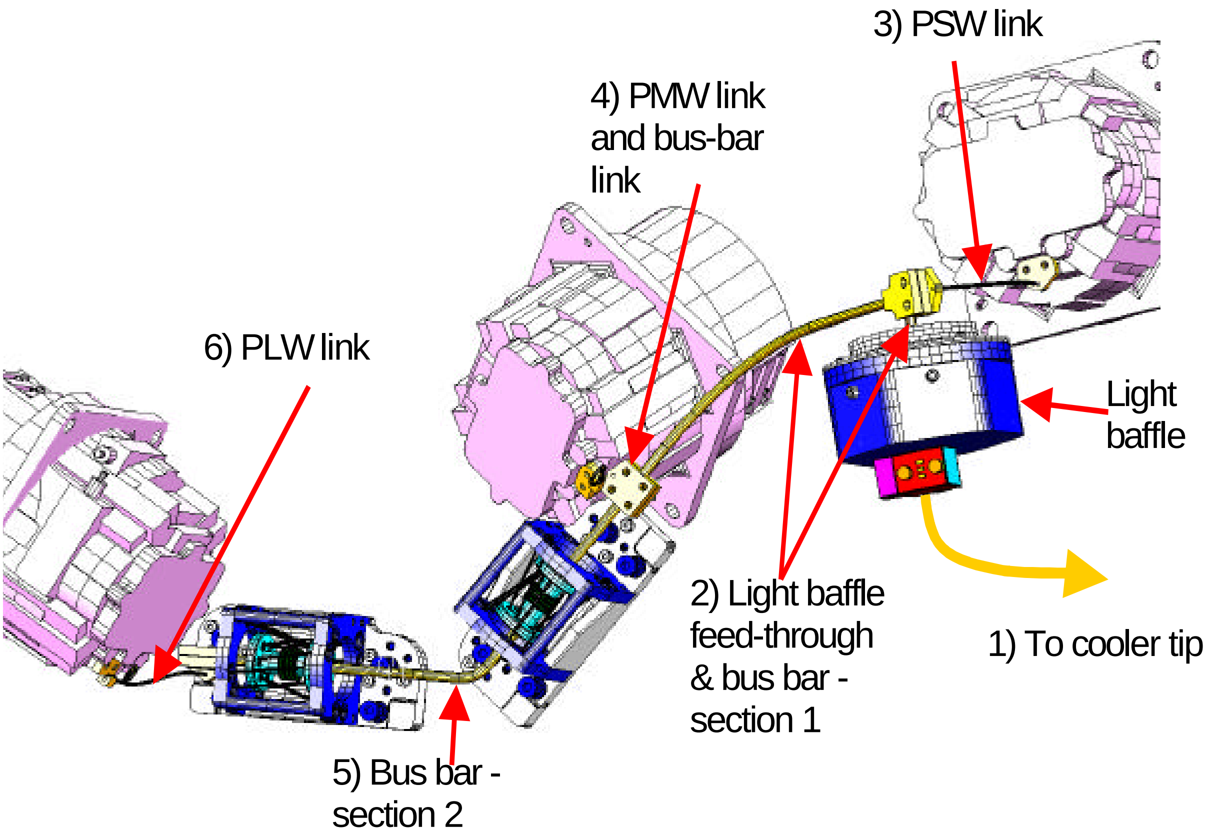

Figure 21 Overview of photometer strap assembly

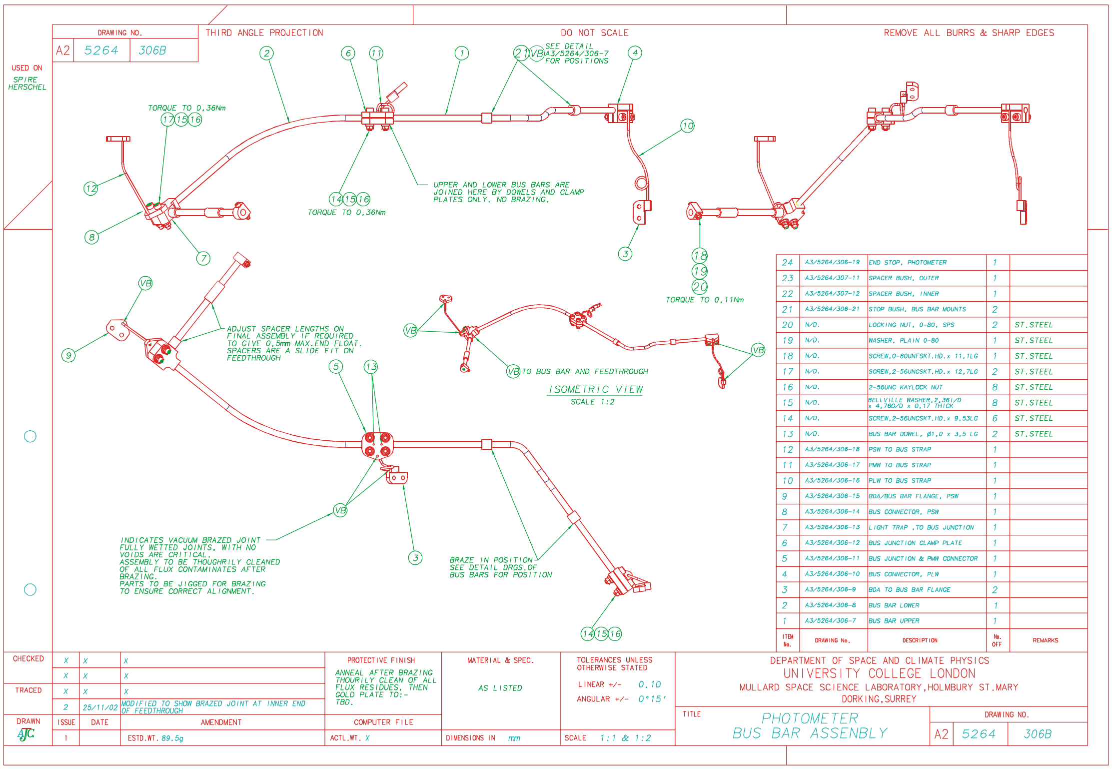

Figure 22 Photometer thermal strap assembly drawing

4.6.2. Interfaces

In the design of the photometer 300mK strap system, we have tried to minimize the number of thermal interfaces while still allowing a reasonable integration sequence. The design of the supports and light baffles is such that only a 3mm diameter rod can be passed through the central hub. This means that the strap assembly must be made in sections, with at least one end having a 3mm rod section that can be passed through the centre of each support. Therefore, several types of thermal interfaces are present in the strap assembly, and are discussed below.

4.6.2.1. Cooler tip interface

The interface to the evaporator cold tip is a copper piece, gold plated 14 mm x 12.5 mm, 3 mm thick, featuring two through holes 3.2 mm in diameter to take two M3 bolts with Belleville washers. Each side of the copper piece is available as a contacting area. A sketch of this interface is shown in Figure 23.

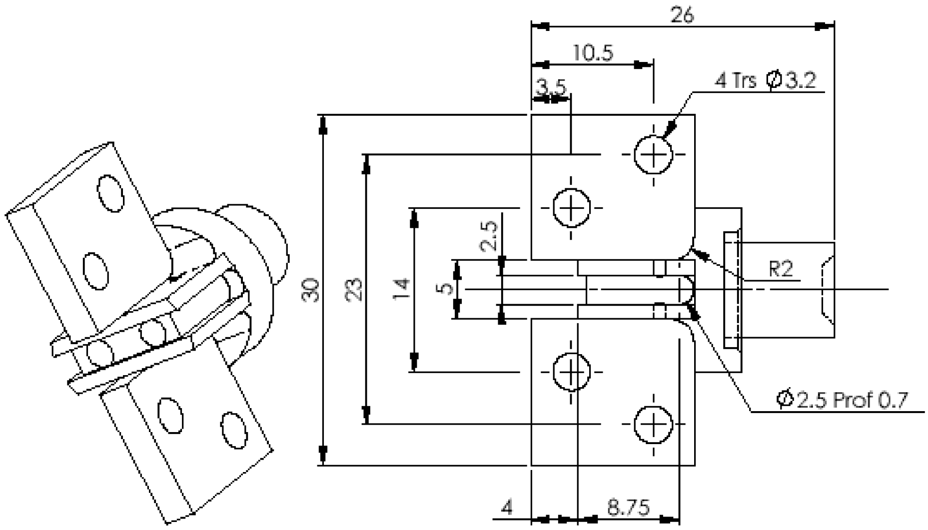

Figure 23 Sketch of cooler tip interface to 300mK straps

4.6.2.2. BDA interface

The interface presented by each BDA consists of a gold-plated copper “tongue” with two M2 clearance holes, below which are two matching M2 tapped holes on the Invar BDA top ring. The 300mK strap interface to the BDA will have matching M2 clearance holes. The interface plate is laid on top of the BDA “tongue” and M2 bolts are passed through both interface plate and tongue and bolted into the Invar top ring. A stack of Belleville spring washers is used for each bolt, and the bolts torqued to 0.21 Nm [RD 4].

4.6.2.3. Rod clamp joint

A clamp joint has been designed, which clamps around the 3mm bar section of each strap component that has to be passed through the central hub of a support or light baffle.

4.6.2.4. Overlapping flat joint

The compliant link to the PSW BDA is bolted to the photometer bus-bar with two bolts clamping flat faces together.

4.6.2.5. Thermal

All 300mK strap components (not including suspension) will be gold plated, and the interfaces will have a surface roughness of TBD rms.
All joints will be made “dry”, i.e. without the use of grease.

4.6.2.6. Electrical

There is a requirement [RD3] for electrical isolation of the photometer and spectrometer strap assemblies from each other, due to the SPIRE grounding scheme. Any electrically isolating joint must have an impedance >1MΩ and a capacitance of <20pF. Of course, it also needs to retain excellent thermal conductivity at 300mK.

The current design under investigation is a directly glued joint, using Stycast 1266 epoxy. A bonding layer of controlled thickness should provide the required electrical parameters while retaining adequate thermal conductivity. Samples have undergone thermal testing at Cardiff University, and are described further in section 5.2. This electrical break (also replicated for the spectrometer strap assembly) will be implemented at the bolted interface to the cooler tip.

4.6.3. Thermal control hardware

There is a possibility that active temperature control may be required for photometer scan map mode. JPL have requested that provision be made for a photometer thermal control (PTC) module which houses three NTD Germanium thermometers and two heaters, and can be bolted to the 300mK strap system. The only location where this could be accommodated is on the "outside" (Level-1 side) of the photometer box stray light baffle. The PTC electrical harness has to run through the RF filters on the spectrometer side of the instrument. The module will be clamped to the 300mK strap as it exits the photometer light baffle on the cooler side, and the harness will run along the photometer strap, via the cooler tip, along the spectrometer strap to a connector mounted off a spine on the spectrometer 2K box. Total parasitics to 300mK from the PTC harness are estimated to be 0.2µW. A schematic of the PTC concept and volume allocation is shown in Figure 24.

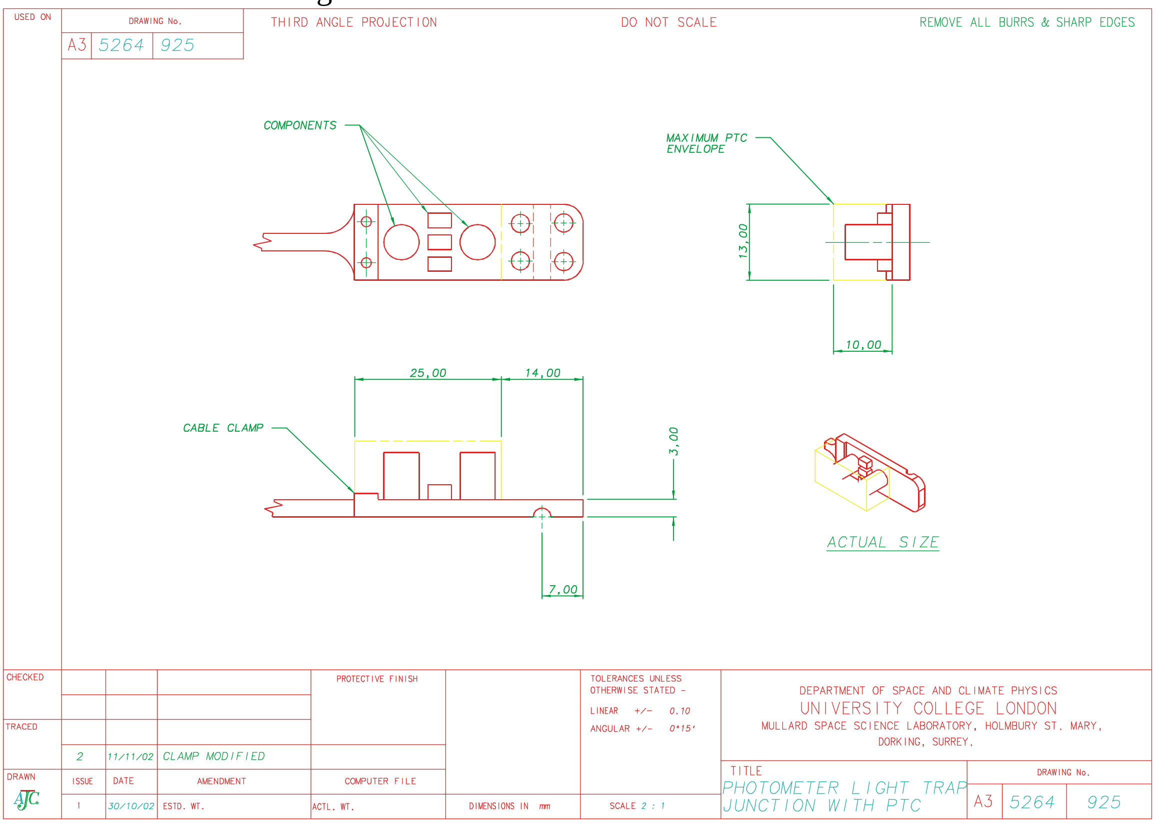

Figure 24 Volume envelope and concept for PTC hardware.

4.7. Spectrometer strap assembly

4.7.1. System overview

Space is extremely restricted within the Level-0 spectrometer detector box. Views of the 300mK system within this box are shown in Figure 25 - Figure 28.
Space restrictions force us to provide additional support for the SLW BDA strap from the SSW BDA clamp, as shown in Figure 27. The additional load on the SSW detector from this arrangement should be minimal. A full FEA is in progress to verify this, and JPL will simulate this arrangement in their warm vibration tests.
The SSW and SLW straps are manufactured from two 1mm diameter gold-plated copper wires, which are permanently fixed (brazed) into interface plates on one end, and into the light baffle feed-through on the other.
The feed from the cooler tip passes through the optical bench and clamps to the spectrometer strap light baffle feed-through. Electrical isolation for this strap will be implemented at the cooler tip. An assembly drawing is shown in Figure 29.

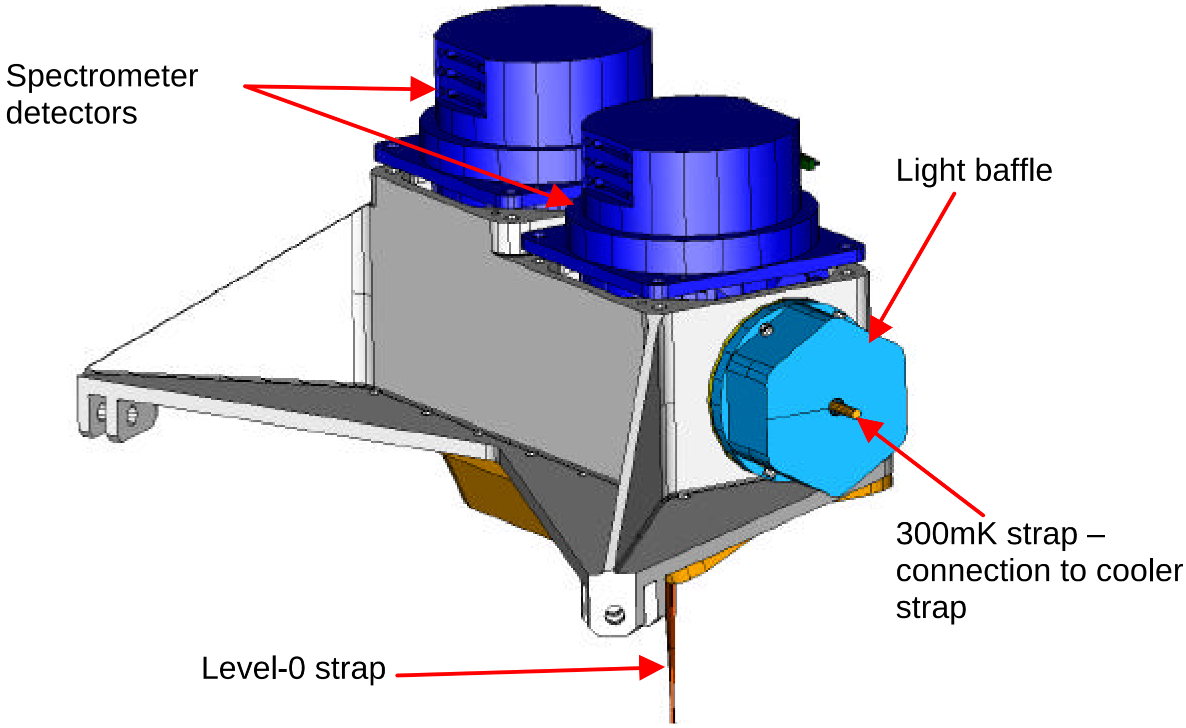

Figure 25 General view of spectrometer Level-0 box with light baffle

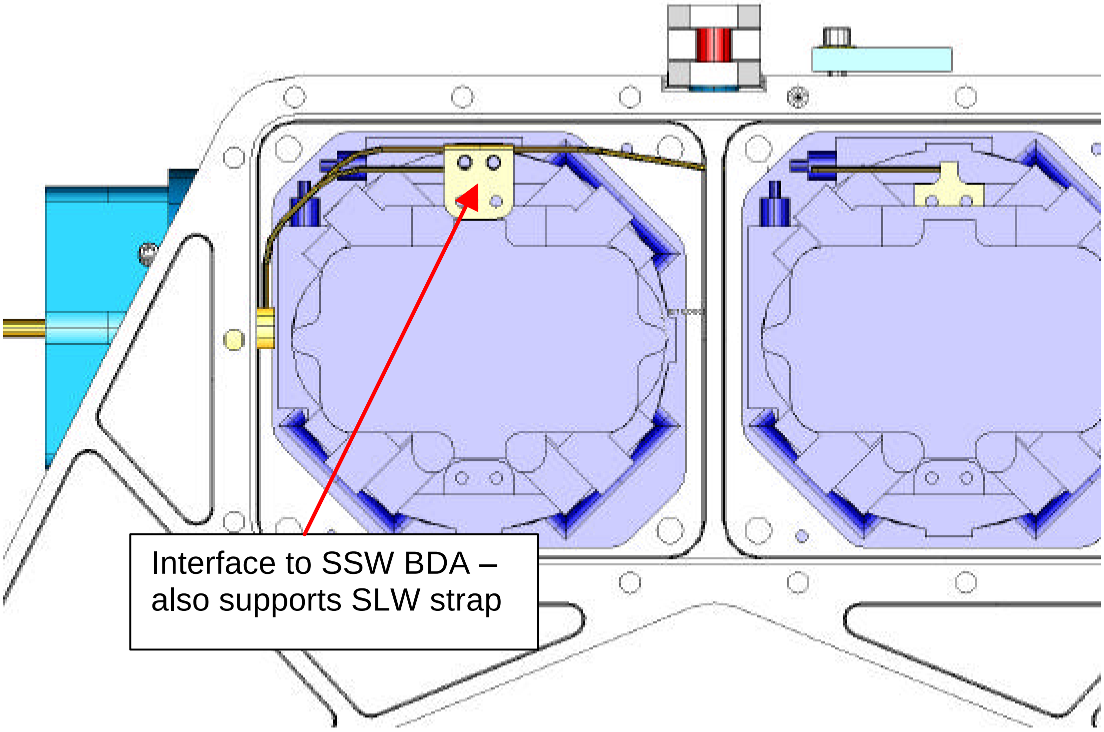

Figure 26 Details of spectrometer 300mK strap routing inside Level-0 box

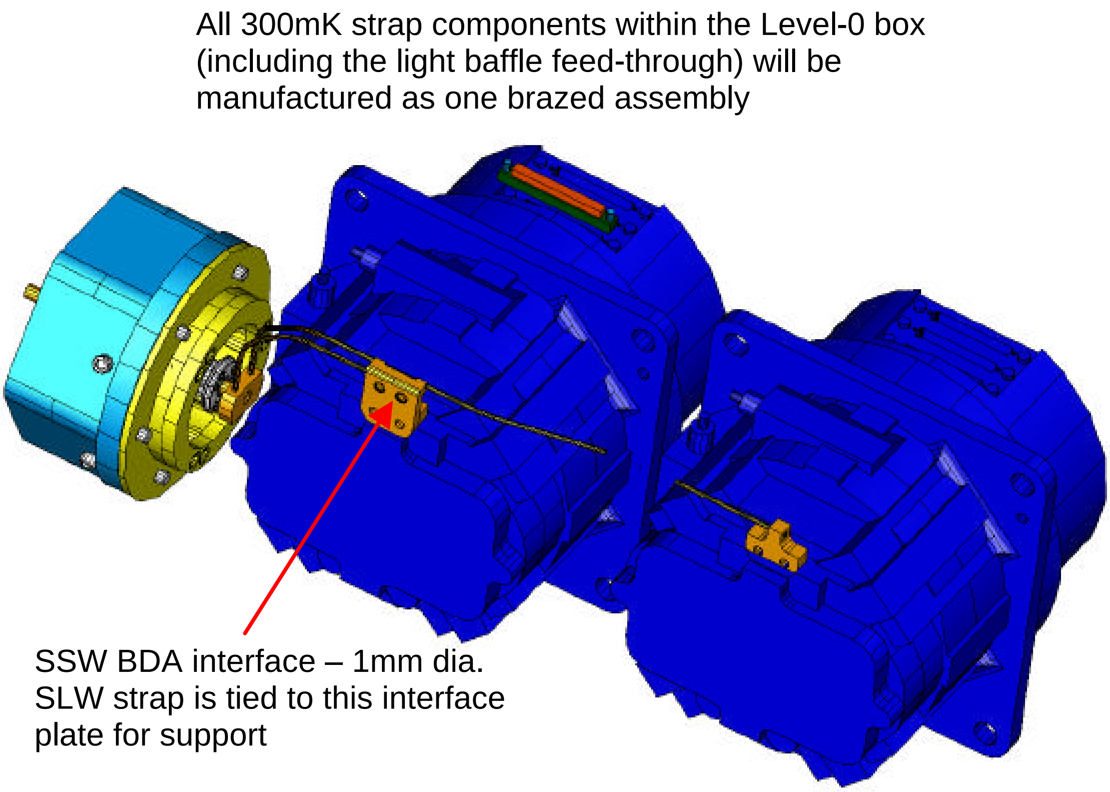

Figure 27 Spectrometer 300mK straps - box removed.

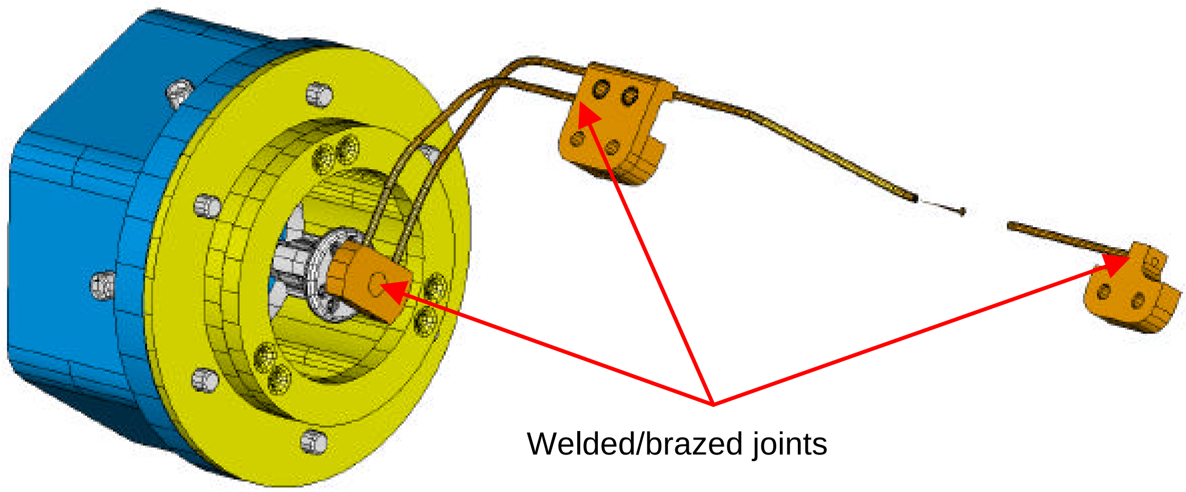

Figure 28 Details of spectrometer 300mK straps

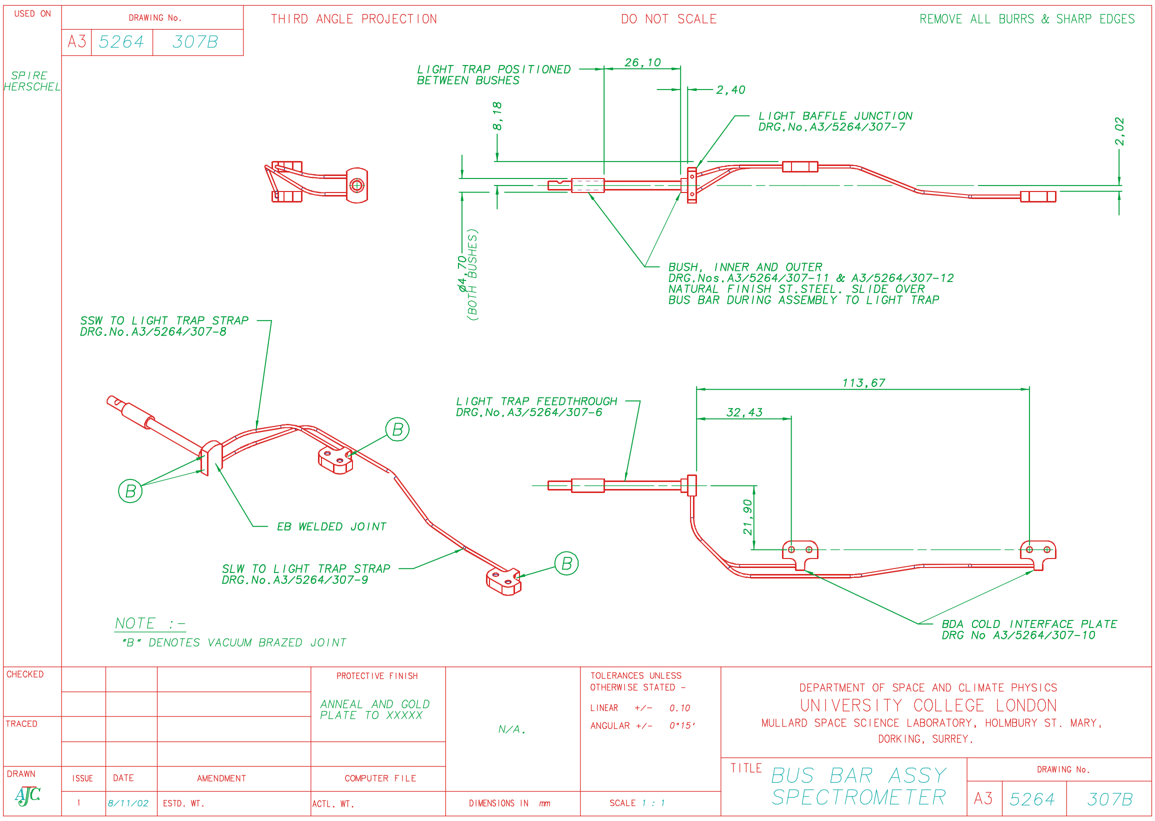

Figure 29 Spectrometer thermal strap assembly drawing

4.7.2. Interfaces

A thermal test campaign has been implemented at Cardiff, which has verified the thermal performance of brazed copper joints at 300mK, and hence validated the design of the spectrometer strap assembly. The interfaces to the spectrometer BDAs are identical to those for the photometer BDAs. Thermal test data is presented in section 5.2.

4.8. Axial constraint of bus-bars

The design of the photometer and spectrometer bus-bar assemblies is such that when assembled, they are fully constrained axially by the photometer supports and light baffles. The hubs are constrained by stainless steel bushes. These bushes only contact the inner hub part, and so do not impede any expansion of the hub, which may take place upon cooling, or as compensation for Kevlar creep. The method employed for constraint at the light baffles is illustrated in Figure 30.

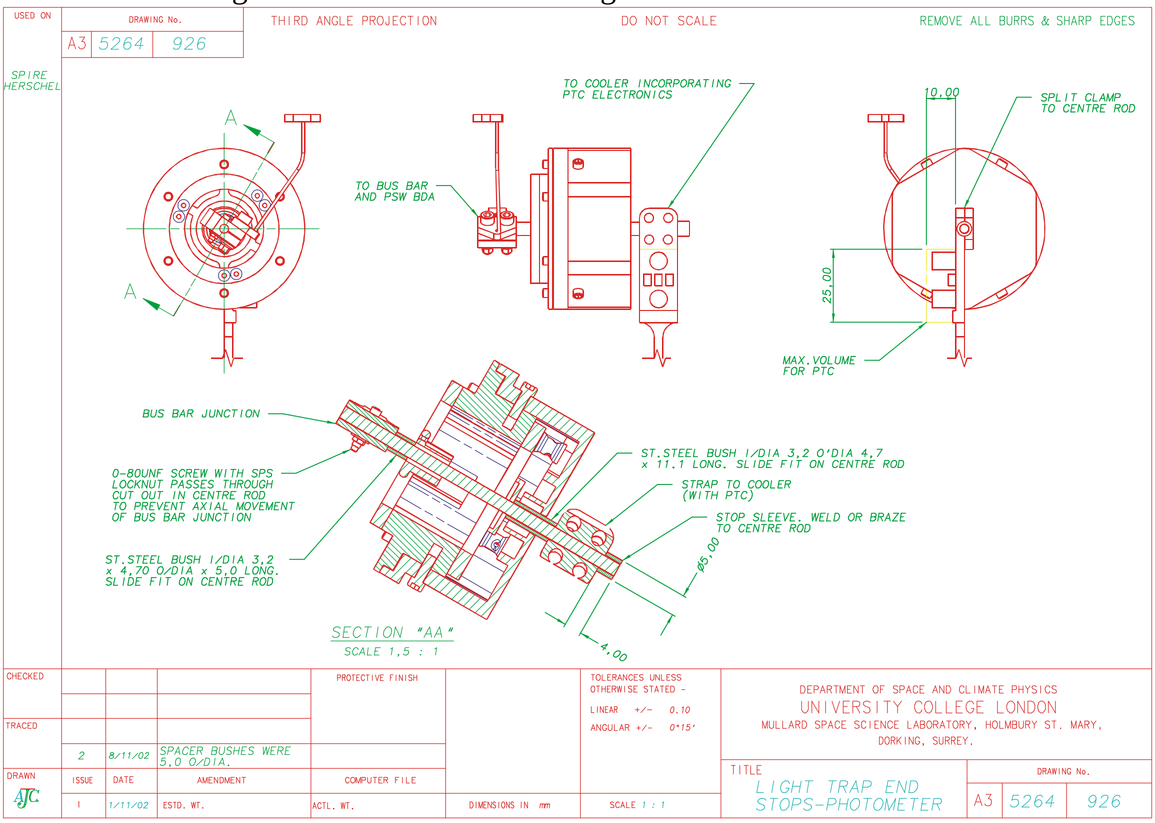

Figure 30 Axial constraint for thermal strap as it passes through the light baffles

The photometer bus-bar is additionally constrained inside the photometer box by the internal bus-bar supports, as shown in Figure 31.

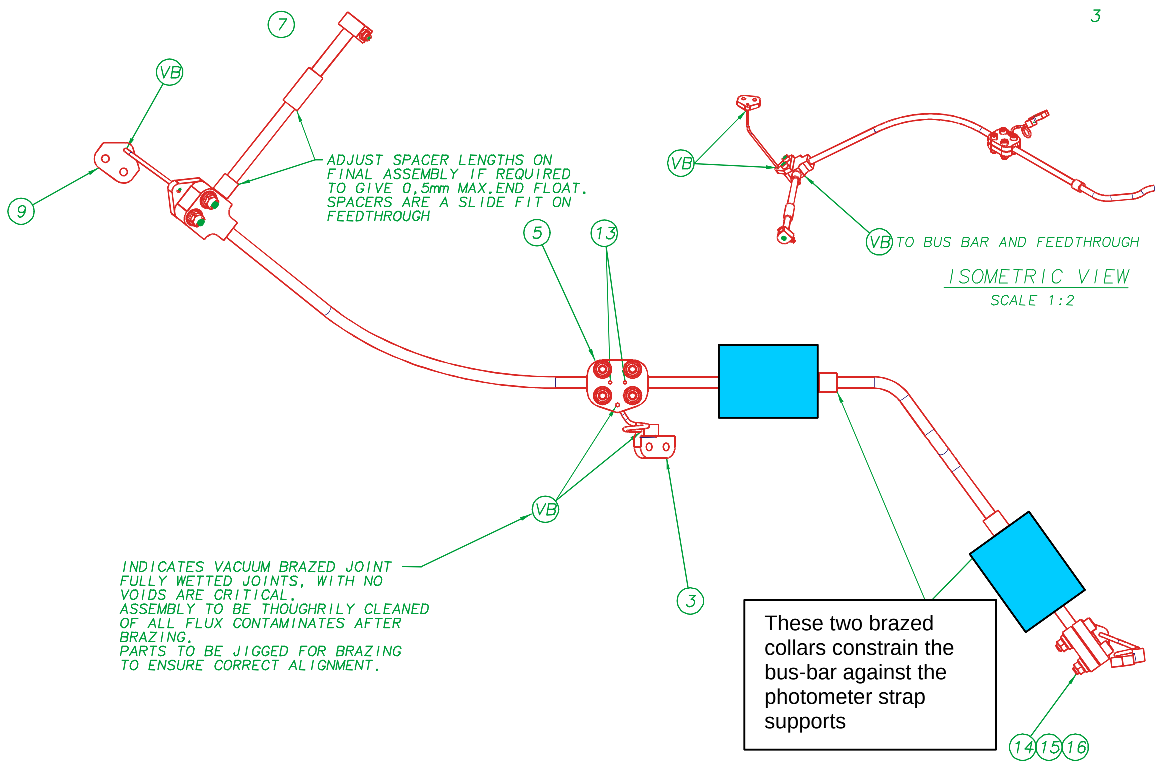

Figure 31 Detail of photometer bus-bar assembly showing method of axial constraint.

5. Test Results

5.1. Mechanical Tests

5.1.1. Warm vibration and FEA

An extensive series of warm vibration tests have been carried out at MSSL, and is summarized in RD5.

5.1.2. Cold vibration

A cold vibration test has been carried out at RAL. A full test report is in preparation at the time of writing this issue, but the main points are summarized below.

5.1.2.1. Test configuration

The test configuration used was as shown in Figure 32. A mechanical mock-up of the photometer strap was built, following guidance from the FEA model of the 300mK system, to impart realistic loads on the single photometer bar support and light baffle.

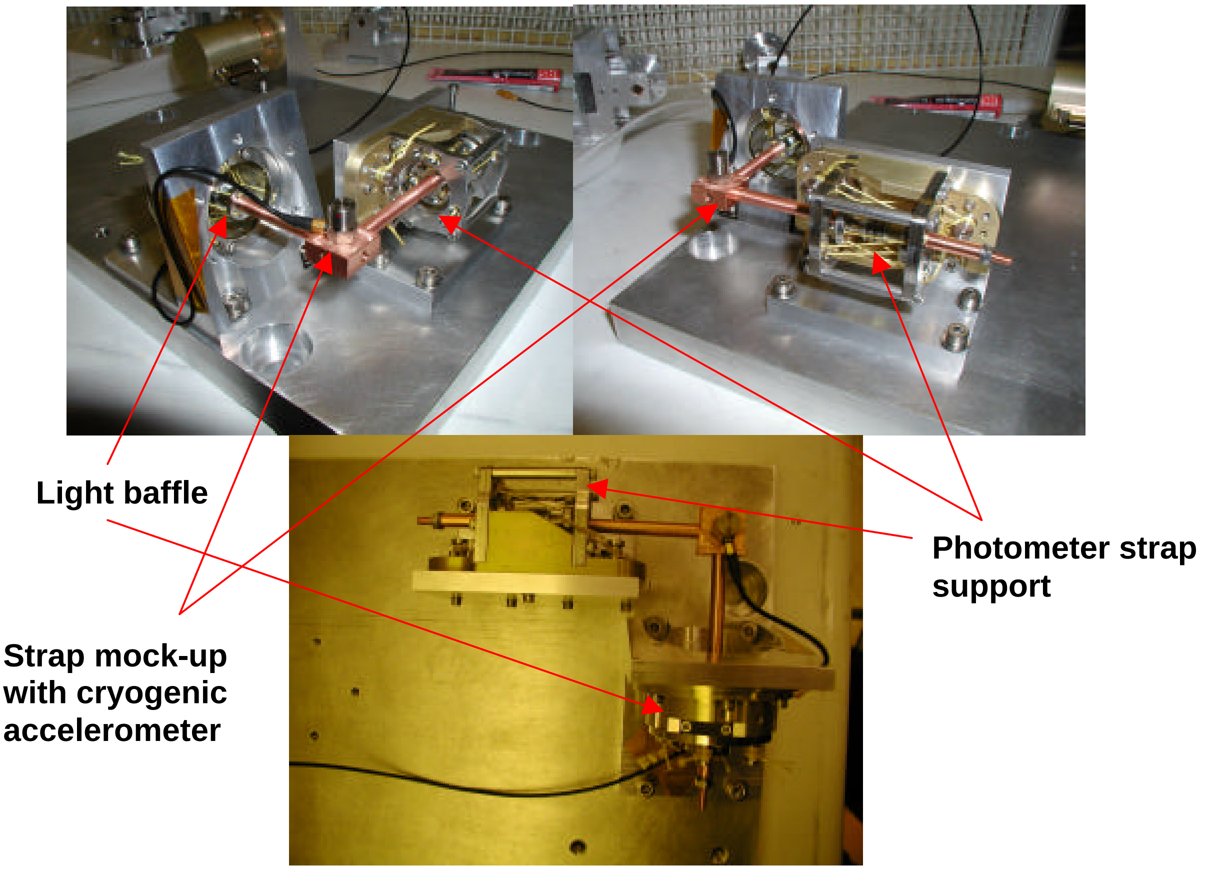

Figure 32 Views of the configuration used for the 300mK system cold vibration test

5.1.2.2. Test sequence

Initially, after mounting the 300mK test components on the shaker interface plate, reasonably accurate (resolution 0.1mm) metrology was conducted to log the positions in space of the points on the bus-bar mock-up indicated in Figure 33.

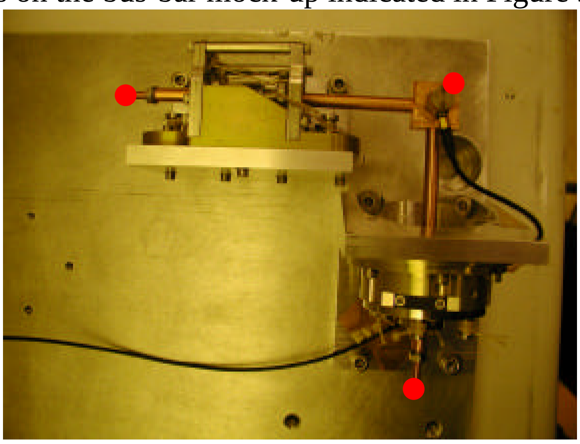

Figure 33 Location of 3D metrology points

After the initial metrology, the interface plate was installed in the cryovibration facility. The following test sequence was then followed:-

- Metrology on the location of the 300-mK suspended components

- Low level sine sweep
- Cool down
- Low level sine sweep
- Quasi static sine qualification
- ½ Power random load for 30 seconds
- Full power random load for 2 minutes
- Low level sine sweep
- Warm up
- Low level sine sweep
- Metrology on the 300-mK suspended components

The random load specification which was applied for this test run was:-

20-100 Hz, +3 dB/oct
100-400 Hz, 0.117 g2/Hz
400-2000 Hz, -12 dB/oct

5.1.2.3. Test results

We present a brief, qualitative summary here. A full report is in preparation at the time of writing.

- The initial warm low-level sine sweep indicated a first mode for the system of 305 Hz
- Upon cooling, the low-level sine sweep indicated that the first mode had INCREASED to 315 Hz. This is thought to be due to the increased Youngs modulus of the Kevlar when cold. It would seem that any increase in the length of the Kevlar upon cooling (observed with the cooler and BDAs) is being adequately compensated for by the Belleville spring stack.
- After the full power sine and random qualification runs, the (cold) first mode frequency was unchanged.
- After warming the system back to room temperature, a low-level sine survey revealed that the first mode frequency had returned to exactly the same "warm" value of 305 Hz.
- Post-shake metrology indicated no measurable shift in the positions of the metrology points.

5.2. Thermal Tests

A series of experiments is, at the time of writing, nearing their conclusion at Cardiff University. Replicas of all thermal interfaces proposed for the 300mK strap system have been manufactured, and the thermal conductivity of each interface has been tested between 300mK and 400mK. Full details can be found in RD6. A summary of the results is simply presented here.

5.2.1. Cooler interface

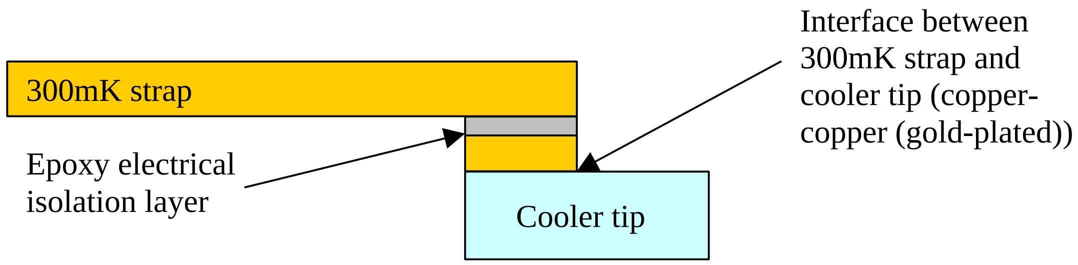

Figure 34 Schematic of cooler tip interface

A replica of the cooler interface has been built and tested in two parts. The conductivity of the copper-copper part of the interface was tested separately to the electrically isolating "epoxy sandwich" part, and the results are shown below. This is because the test components were built prior to the requirement for electrical isolation being implemented. A complete replica of the cooler interface in manufacture at Cardiff, and the interface will be tested as a single unit.

5.2.1.1. Non-electrically isolating part

A test of a gold-plated copper to gold-plated copper pressed interface was made, to replicate the cooler side of the epoxy sandwich. The joint was made "dry", i.e. no grease was used. The configuration is shown in Figure 35.

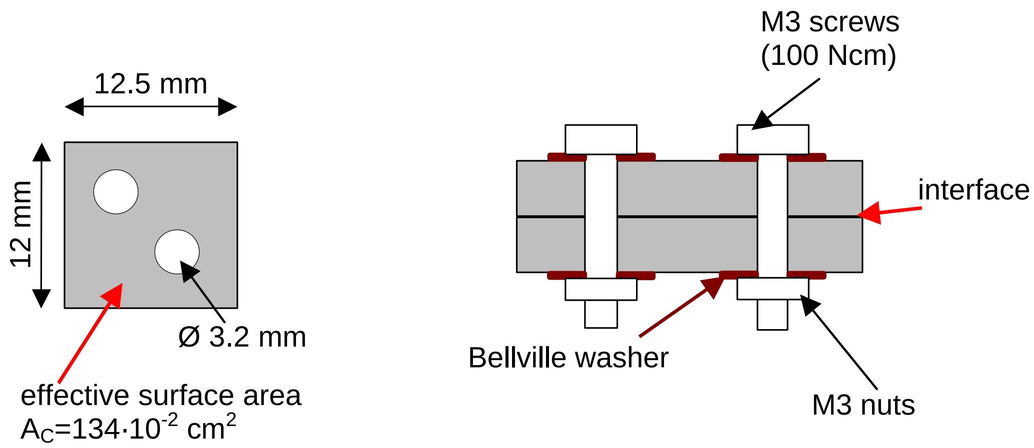

Figure 35 Cooler non-isolating interface thermal test configuration

Test results are shown in Figure 36. This measurement was repeated three times after de-mounting & re-mounting the joint between each measurement. The data was highly repeatable.

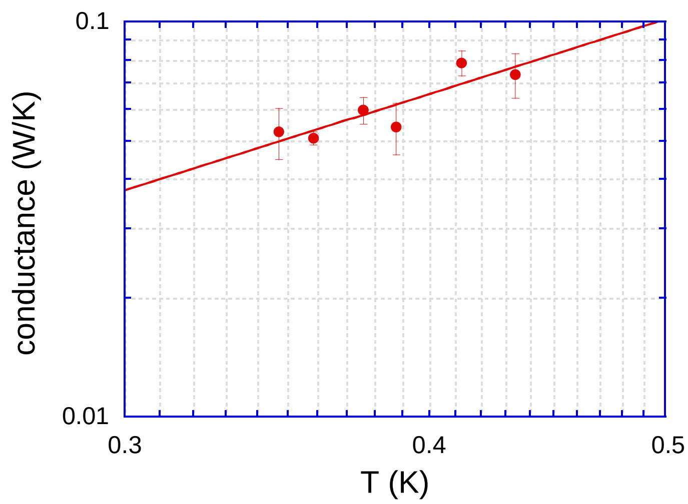

Figure 36 Thermal conductance of copper-copper part of cooler interface. Data can be can be fitted by $G = 0.392 \cdot T^{1.952}$.

5.2.1.2. Epoxy isolation joint

This joint is made using a 150 micron layer of Stycast 1266. The test configuration is shown in Figure 37 and the results are shown in

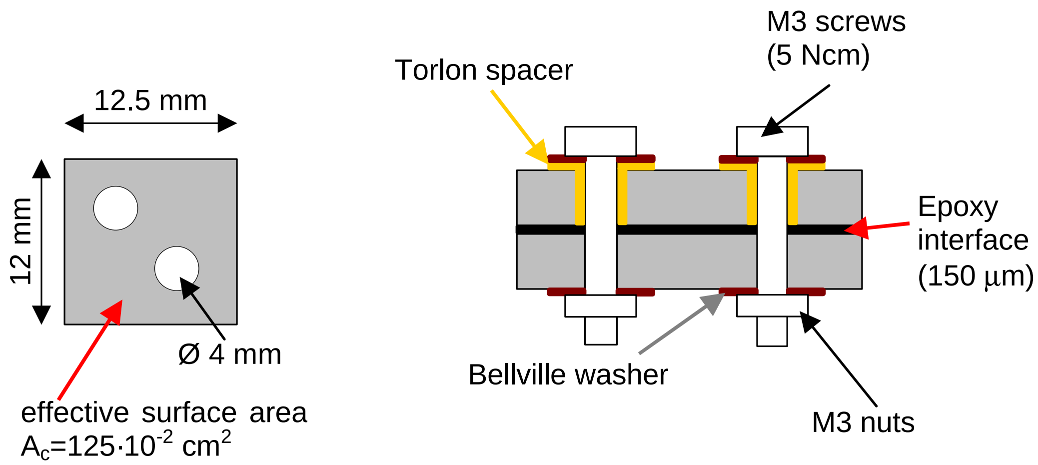

Figure 37 Configuration for thermal test of epoxy electrical isolation joint

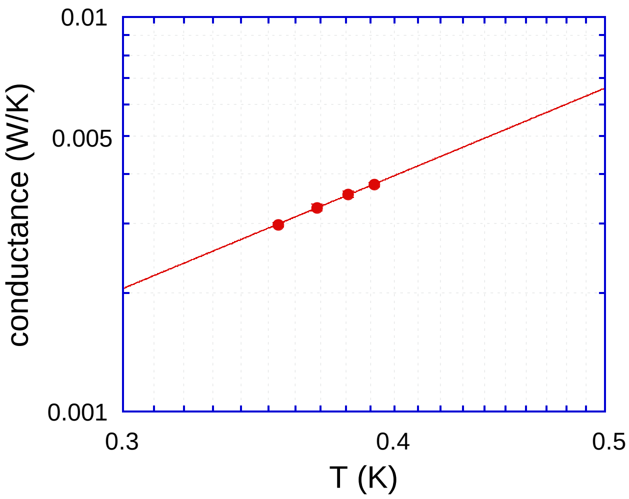

Figure 38 Thermal conductance for epoxy isolated section of cooler interface. The data can be fitted by $G = 3.228 \cdot 10^{-2} \cdot T^{2.2889}$.

5.2.2. Two-part bus-bar clamp joint

This joint replicates the joint between the upper and lower bus-bars in the photometer box.

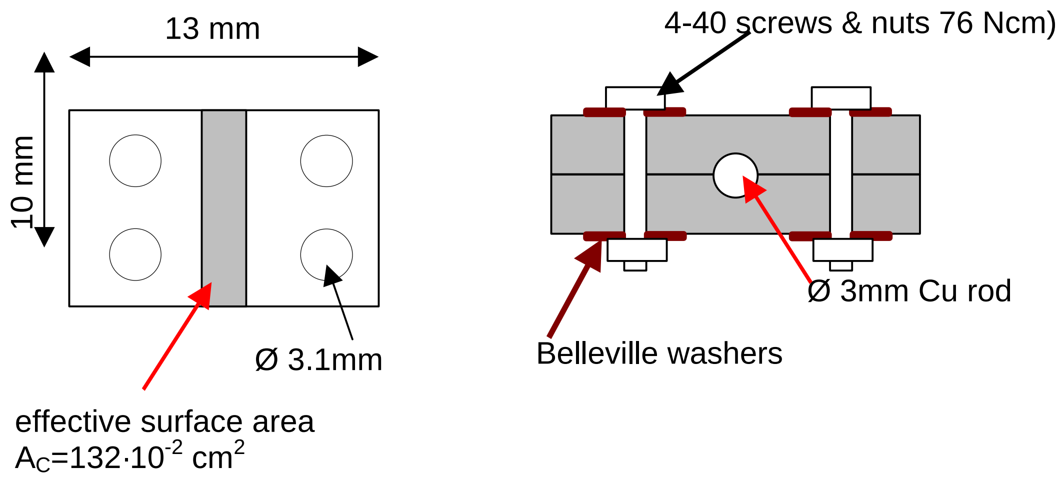

Figure 39 Thermal test configuration of two-part bus-bar clamp joint

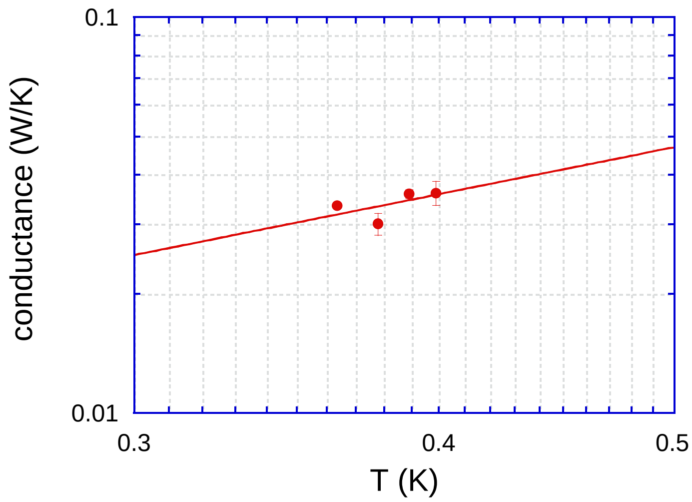

Figure 40 Thermal conductance of two-part bus-bar clamp joint. Data can be fitted by

$$G = 0.11 \cdot T^{1.2295}.$$

5.2.3. "C-type" round bus-bar clamp interface

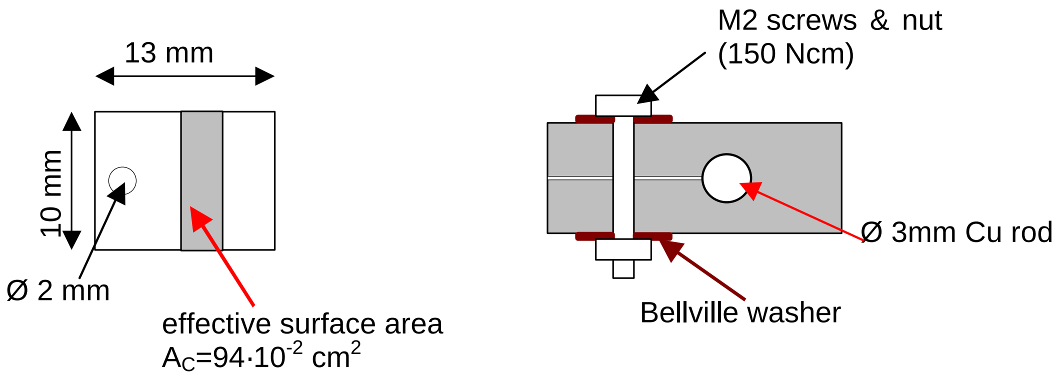

Figure 41 Thermal test configuration of "C-type" round bus-bar clamp interface

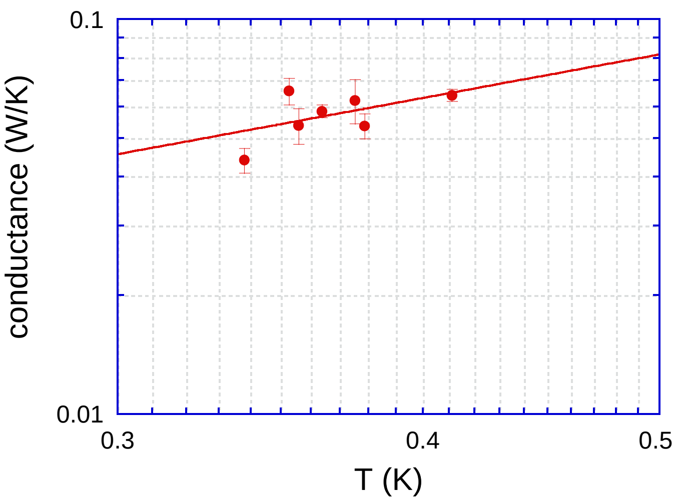

Figure 42 Thermal conductance of C-type clamp joint. Data can be fitted by

$$G = 0.1794 \cdot T^{1.1395}.$$

5.2.4. BDA interface

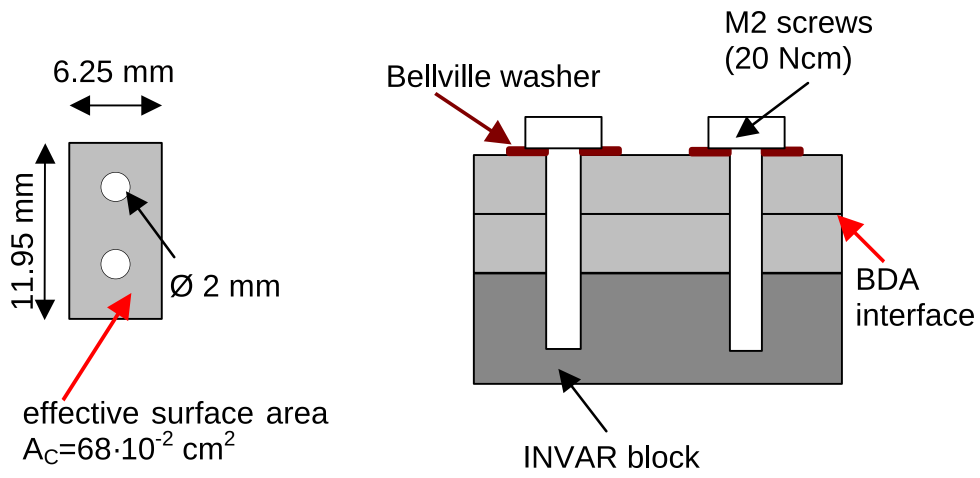

Figure 43 Thermal test configuration for BDA interface replica

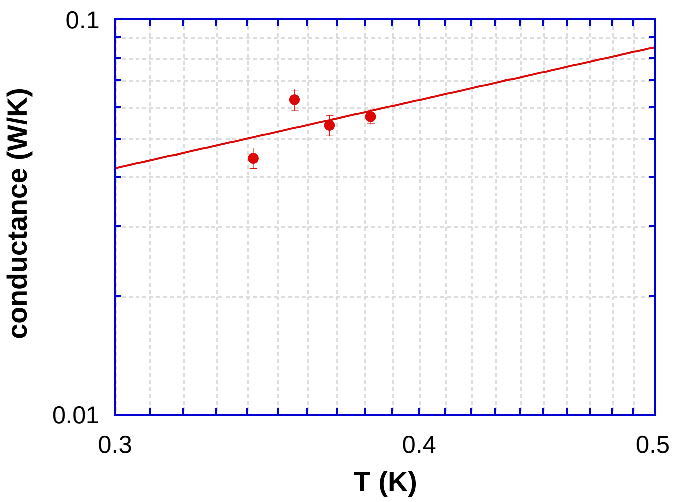

Figure 44 Thermal conductance of BDA interface replica joint.

5.2.5. Brazed joint verification

There was uncertainty as to whether sections of the bus-bar assembly should be brazed or e-beam welded with regard to their thermal performance at 300mK. Brazing is the preferred assembly method, as e-beam welding would be very difficult for where a 1mm diameter wire is fixed into a copper block. Therefore, a test component was built at MSSL according to their in-house brazing procedure, and tested at Cardiff. The component is shown in Figure 45.

Thermal test results are shown in Figure 46. This graph compares the conductivity of the whole assembly with brazed joints to the conductivity that the assembly would have if it were machined from just one block of copper of various grades. The conductivity of the assembly is the same as the conductivity of bulk copper, therefore it can be concluded that the MSSL brazing procedure is perfectly adequate for use in the SPIRE bus-bar assembly.

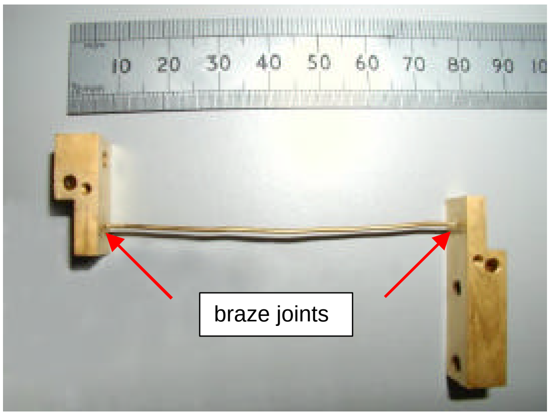

Figure 45 Test component manufactured at MSSL to check performance of brazed joints at 300mK

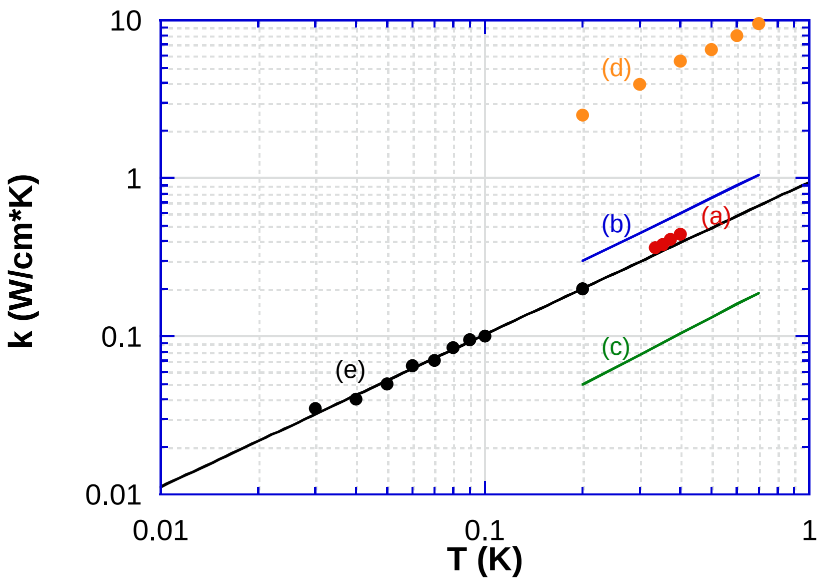

Figure 46 Comparison of thermal conductivity of several Copper sample which differ in degree of purity. (a) Brazed busbar manufactured at MSSL: (b) Cu, RRR=100; (c) Cu, RRR=20 (R.L. Garwin, Rev. Sci. Instr. 27 (1956)); (d) pure Cu, impurities less than < 10 ppm; (e) commercial pure Cu (Lounasmaa: "Exp. Principles and Methods below 1K)

6. References

1. "Experimental characterization of Kevlar 29". TNS4, Issue 0 Rev. 1. L. Duband
2. Duband et al - Cryogenics 33, no6 643-64
3. Ventura et al – Cryogenics 40 (2000) 489-491